ACCSCIENCE PUBLISHING

International Journal of Bioprinting

REVIEW ARTICLE

Extracellular matrix-inspired 4D SMART biomaterials for bioprinting in tissue engineering

Ryan Martin[1], Haiwei Zhai[2], Daehoon Han[3], Fanben Meng[2,4]*, and Daeha Joung[1,5]*

[1]Department of Physics, College of Humanities and Sciences, Virginia Commonwealth University, Richmond, Virginia, United States

[2]Department of Mechanical and Materials Engineering, College of Engineering, University of Nebraska-Lincoln, Lincoln, Nebraska, United States

[3]School of Chemical Engineering, Chonnam National University, Gwangju, Republic of Korea

[4]Nebraska Center for Integrated Biomolecular Communication, University of Nebraska-Lincoln, Lincoln, Nebraska, United States

[5]Massey Comprehensive Cancer Center, Virginia Commonwealth University, Richmond, Virginia, United States

(This article belongs to the *Special Issue*: *Multidisciplinary Efforts in Bioprinting*)

Abstract

Tissue development and regeneration arise from a dynamic interplay among cells, the extracellular matrix (ECM), and surrounding biophysical and biochemical cues. These interactions form the basis for stimuli-responsive materials for advanced regenerative technologies (SMART) that drive innovation in four-dimensional (4D) bioprinting for tissue engineering. This review discusses the biophysical foundations of SMART materials, emphasizing native ECM components, their interactions, and organ-specific properties that inform biomimetic material design. We highlight recent advances in 4D SMART systems, including ionic self-healing, pH-, thermal-, hydration-, and magneto-responsive materials, and their roles in mimicking developmental and regenerative processes. This is followed by a comparative overview of these stimuli-responsive material classes, benchmarked against one another, native ECM performance, and clinical translation requirements, revealing persistent gaps in long-term stability, multi-stimuli integration, and regulatory feasibility. Together, these insights provide an interdisciplinary framework for designing adaptive, responsive biomaterials that guide tissue morphogenesis and advance the future of regenerative medicine.

Keywords: Biomaterials; Extracellular matrix; Four-dimensional bioprinting; Four-dimensional tissue engineering; Regenerative medicine; Stimuli-responsive materials

***Corresponding authors:**
Fanben Meng
(fmeng5@unl.edu)

Daeha Joung
(joungd2@vcu.edu)

Citation: Martin R, Zhai H, Han D, Meng F, Joung D. Extracellular matrix-inspired 4D SMART biomaterials for bioprinting in tissue engineering. *Int J Bioprint*. 2026;12(1):225-261. doi: 10.36922/IJB025440447

Received: October 29, 2025
1st revised: December 6, 2025
2nd revised: December 17, 2025
Accepted: December 26, 2025
Published online: January 12, 2026

1. Introduction

Extracellular matrix (ECM) has reigned as biology's unrivaled, living four-dimensional (4D) engine—continuously self-remodeling over seconds to decades, reversibly

stiffening and softening via closed-loop signaling with cells, thereby directing multicellular organization and scarless regeneration.[1] In an effort to recapitulate ECM dynamics, researchers have developed stimuli-responsive materials for advanced regenerative technologies (SMART), which represent a multidisciplinary convergence of chemistry, physics, engineering, and biomedicine aimed at addressing complex challenges in tissue regeneration, disease modeling, and therapeutic innovation. By integrating time (temporal dynamics) as the fourth dimension, these developments have paved the way for 4D bioprinting and 4D tissue engineering. When combined with SMART materials, these emerging approaches show strong promise for enabling safer and less invasive clinical interventions.[2,3]

However, current 4D SMART materials still rely on abiotic, one-shot triggers that bear no resemblance to the ECM's biotic, reversible, and multi-cycle dynamics driven by cell-secreted enzymes, traction forces, and redox state.[4–6] Because current materials cannot continuously turn over, expose fresh ligands, or reversibly re-crosslink in response to ongoing cellular cues—the very mechanisms that keep native ECM recognized as intrinsic to the body and fibrosis-free—they remain mechanically incompetent, immunologically provocative, and biologically obsolete long before any clinically meaningful regeneration can occur.[7] Consequently, the field has reached an inflection point, where establishing yet another single-trick material or platform is no longer defensible as "progress." Instead, absolute ECM fidelity must now be adopted as the non-negotiable standard and primary metric of success, requiring that next-generation 4D platforms exhibit continuous molecular turnover, cell-controlled reversible crosslinking, release of anti-fibrotic matrikines, strain-rate-matched viscoelasticity, and sustained immunological silence before they can be considered candidates for clinical translation.[8]

To bridge this gap, contemporary SMART material development integrates interdisciplinary advances to recapitulate seven key hallmarks of living tissues: biomimetic composition, multi-stimuli responsiveness, spatiotemporal heterogeneity, mechano-reciprocity, bioactive signaling, immunomodulation, and vascularization.[7,9,10] Biological insight—particularly into cellular mechanotransduction, self-organization, and differentiation—guides this effort, while chemical innovation enables dynamic bioinks and cross-linkers capable of programmed, time-evolving mechanics and biochemical responses. Physics provides precise control over internal and external cues (e.g., mechanical constraints, optical triggers, and acoustic fields) that orchestrate shape morphing, cell–matrix dialog, and biomechanical fidelity.[9–11] Finally, engineering optimizes bioreactor platforms and stimulus-delivery systems to ensure scalability and clinical translatability.[12–15] This convergent framework for achieving ECM fidelity through these seven key hallmarks aims to transform SMART materials into truly biomimetic 4D constructs poised for regenerative medicine.

Before delving into the critical assessment of the field, it is essential—given the inherently interdisciplinary nature of 4D bioprinting and 4D tissue engineering—to clarify foundational concepts and terminology that enable effective collaboration across specialties. 4D bioprinting extends conventional three-dimensional (3D) bioprinting, including extrusion-, inkjet-, stereolithography-, laser-assisted, or volumetric techniques—in which living cells are precisely deposited within biocompatible hydrogels or bioinks—by incorporating stimuli-responsive materials (SRMs) that confer time-dependent structural and functional evolution to the printed construct.[16] Following fabrication, these SMART materials undergo programmed or stimuli-triggered transformations (e.g., shape change, stiffness modulation, or matrix remodeling) in response to physiological, biochemical, or external cues, more faithfully recapitulating the spatiotemporal complexity of the native ECM and its active role in directing cell fate, tissue morphogenesis, and organ-level function.[15,17,18]

In contrast, 4D tissue engineering represents a broader paradigm that encompasses all time-dependent strategies for creating dynamically evolving constructs, irrespective of fabrication method. While this includes bioprinting-based approaches, the term is used in this review to also encompass non-bioprinting techniques—such as scaffold-free cellular self-assembly, constructs incorporating embedded responsive molecules, or the direct application of external physical stimuli (e.g., acoustic fields, mechanical vibration, magnetic forces, or fluid shear). In every instance, programmed temporal transformations are driven by endogenous biochemical cues or externally applied stimuli. These changes facilitate mechanotransduction, structural remodeling, functional maturation, and phenotypic specification, as reflected by alterations in cell morphology, behavior, or biochemical profiles.[11,19]

The SMART materials are advanced, multifunctional composites designed to actively sense and transduce environmental cues into programmable physicochemical changes, thereby establishing bidirectional, dynamic reciprocity with embedded cells and tissues. At the molecular level, these materials incorporate responsive motifs—such as thermoresponsive poly(*N*-isopropylacrylamide) (PNIPAAm) chains, photo-cleavable o-nitrobenzyl groups, pH-sensitive ionizable moieties, enzyme-cleavable peptide linkers, or mechanotransductive

crosslinkers—whose conformational transitions or bond scission events trigger macroscopic property shifts.[5,6] These shifts include reversible or irreversible modulation of storage and loss moduli (often spanning 10 Pa to over 100 kPa), viscoelastic creep compliance, hydraulic permeability, mesh size, ligand tether mobility, and cryptic domain exposure.[20] By coupling such biophysical outputs to cellular force generation (typically 10–10,000 nN per cell), SMART materials recapitulate key ECM feedback loops: force-dependent stiffening/softening, stress–relaxation-driven lineage commitment, durotaxis, and matrix metalloproteinase (MMP)-mediated remodeling.[9,15,20–22]

Within 4D bioprinting for tissue engineering, these materials enable precise spatiotemporal orchestration of morphogenesis, such as sequential unfolding or folding, gradient stiffening mimicking embryonic condensation, or on-demand release of growth factors and signaling molecules. Emerging electroactive subclasses—such as piezoelectric polyvinylidene fluoride (PVDF) composites, conducting polymers, including poly(3,4-ethylenedioxythiophene):polystyrene sulfonate (PEDOT:PSS) and polyaniline (PANI), and carbon-nanotube-reinforced hydrogels—enable the transduction or application of electric fields (0.1–100 mV mm^{-1}), supporting electromechanical coupling critical for cardiac, neural, and musculoskeletal tissues.[23,24] This convergence of mechanical, chemical, and electrical responsiveness positions SMART materials as essential platforms for interrogating developmental mechanobiology, engineering load-bearing tissues, and constructing organoids that faithfully recapitulate in vivo patterning dynamics.[15,25]

Native ECMs serve as the principal inspiration for SMART biomaterial design in 4D tissue engineering through two interconnected mechanisms. First, the core biophysical and biochemical principles of the ECM—such as dynamic stiffness modulation, viscoelasticity, spatially patterned ligand presentation, force-dependent cryptic site exposure, and protease-mediated remodeling—directly

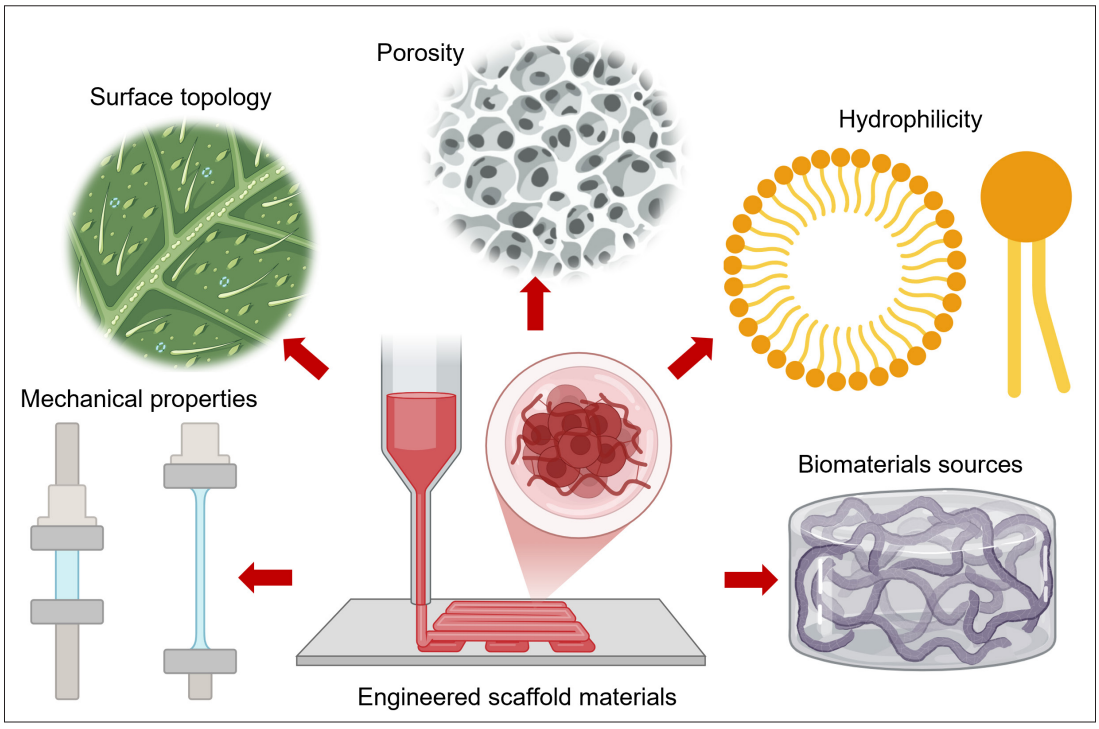

Figure 1. Biophysical traits of stimuli-responsive materials for advanced regenerative technologies (SMART) materials in tissue engineering and bioprinting. This schematic illustration highlights the core properties of stimuli-responsive biomaterials that dynamically emulate the native extracellular matrix (ECM). Five key attributes branch from the central SMART scaffold: (i) surface topology: micro- and nanoscale patterns, roughness, and fibrous structures that replicate ECM textures; (ii) mechanical properties: tunable stiffness (0.1–1 kPa for soft tissues like brain; 10–100 kPa for rigid tissues like bone), elasticity, viscoelasticity, and tensile strength; (iii) porosity and architecture: 50–90% interconnected porosity forming three-dimensional frameworks analogous to the hydrated, porous ECM gel; (iv) hydrophilicity: wettability and water retention that mimic the glycosaminoglycan-rich ECM environment; (v) biomaterial source: natural (e.g., collagen, chitosan) providing bioactivity and RGD (arginine–glycine–aspartic acid) signaling motifs; synthetic (e.g., polycaprolactone, polylactic acid) enabling precise customization and controlled degradation; or hybrid (e.g., decellularized ECM combined with polyethylene glycol), balancing biodegradability, bioactivity, and reduced immunogenicity. Created in BioRender. Joung, D. (2025). https://BioRender.com/bt3s7z1.

inform the engineering of stimuli-responsive "SMART" materials.[26] These principles are translated into synthetic or hybrid composites that recapitulate tunable mechanics, degradability, and bioactivity, thereby enabling precise regulation of cell traction forces, mechanotransduction pathways, and cell fate decisions.[26,27]

Second, the ECM's inherent spatiotemporal dynamism actively guides the development of SMART materials by providing a blueprint for their programmed evolution over time. The ECM undergoes continuous maturation, stiffening, and topographic reconfiguration during development and repair. Replicating these time-dependent transitions has driven the incorporation of stimuli-responsive polymers, shape-memory components, and cell-mediated remodeling cues into 4D platforms. This ensures that printed or assembled constructs do not remain static but instead mature, fold, stiffen, or functionally specialize in synchrony with resident cells—mirroring morphogenetic and homeostatic processes observed *in vivo*.[22,28] Thus, ECM-derived design rules elevate SMART biomaterials from passive structural supports to active, instructive participants in tissue morphogenesis.

By orchestrating tissue development, homeostasis, and regeneration through a suite of interdependent biophysical traits: the ECM possesses organ-specific biochemical composition, tunable stiffness and viscoelasticity, hierarchical surface topography, interconnected porosity and 3D architecture, and finely regulated hydrophilicity (Figure 1).[29–31] Each of these features defines tissue functionality from early development through maturation and regeneration.

Surface topology defines the microstructural interface of materials, ranging from aligned collagen fibrils and basement-membrane nanoridges that provide contact guidance, to microscale roughness that governs initial protein adsorption and cell spreading.[28,32] Mechanical properties, such as stiffness and viscoelasticity, allow biomaterials to approximate physiological moduli (1–100 kPa for soft tissues) and thereby transmit forces to cells and drive mechanotransduction via integrin clustering and Yes-associated protein (YAP)/transcriptional coactivator with PDZ-binding motif (TAZ) nuclear shuttling.[33–36] Interconnected porosity (typically 50–500 μm pores) and 4D architecture establish diffusion gradients for oxygen, nutrients, and waste while permitting cell migration and vascular ingrowth.[37] Hydrophilicity reflects a material's water-attracting capacity, conferred by hydroxyl, carboxyl, and sulfate groups, and maintains hydration, stabilizes adsorbed protein conformation, and facilitates integrin-mediated adhesion.[28] Collectively, these biophysical cues, along with the biomaterial source (natural, synthetic, or hybrid), render the ECM a dynamic, instructive microenvironment that actively regulates cell fate, tissue morphogenesis, and functional restoration.[28,38]

Current ECM-derived and ECM-inspired biomaterials for bioprinting and tissue engineering encompass native structural and adhesive proteins (e.g., collagen type I/IV, fibrin), glycosaminoglycans (GAGs; e.g., hyaluronic acid [HA], heparan sulfate [HS]), decellularized ECM (dECM) from various tissues, semi-synthetic hybrids (e.g., gelatin-methacryloyl [GelMA], methacrylated HA [HAMA], thiolated/norbornene-modified HA), and fully synthetic mimics (e.g., polyethylene glycol [PEG]-based peptide conjugates, polycaprolactone [PCL]/PEG block copolymers).[39–41] Although these materials recapitulate baseline ECM features—including ligand identity (e.g., RGD, isoleucine–lysine–valine–alanine–valine [IKVAV], tyrosine–isoleucine–glycine–serine–arginine [YIGSR]), fibrillar topography, initial viscoelasticity, and protease-dependent degradability—their storage moduli (G'), loss moduli (G"), stress–relaxation timescales, mesh size, and ligand presentation remain essentially fixed post-fabrication, thereby failing to capture the profound temporal evolution observed *in vivo*.[42]

In contrast, ECM-derived SMART materials engineer true dynamic reciprocity by building directly upon native or bio-orthogonal ECM chemistries, actively emulating the physiologically relevant viscoelastic spectrum, force-dependent ligand uncaging, traction-mediated remodeling, and spatiotemporal bioactive epitope gradients of developing and healing tissues, thereby transforming conventional ECM mimics into temporally evolving, instructive matrices that orchestrate morphogenesis in 4D bioprinted and bioassembled constructs.[43]

While previous review articles have provided overviews of 4D printing with SMART materials, focusing on applications in wearable devices, soft robotics, and tissue engineering, they typically survey established technologies and highlight niche challenges.[44,45] In contrast, this review uniquely integrates ECM-derived insights across subfields to establish a new biomimetic framework for future 4D SMART material development in bioprinting, emphasizing the inherent dynamic properties of ECM components that the field implicitly seeks to replicate. We first explore the core biophysical, biochemical, and organ-specific mechanisms of the ECM that should now serve as the uncompromising blueprint for all future biomaterial design. Then, we examine the activation mechanisms in current SMART materials, their applications in mechanistic research, and potential for clinical translation, followed by a comparative review of each stimulus approach. We conclude by outlining emerging directions and remaining

challenges in developing adaptive, next-generation materials for regenerative medicine.

2. Biophysical foundation of SMART materials

2.1. Extracellular matrix components and their cellular interactions

The ECM serves as a dynamic blueprint for engineering 4D SMART materials, offering explicit, translatable design rules derived from native biophysical and biochemical cues that profoundly shape cellular attributes such as orientation, stiffness, contractility, and polarity through topographic features, substrate rigidity, and ligand density.[46,47] Topographic alignment can be replicated using electrospun fibers (200–800 nm diameter) or microgrooved polydimethylsiloxane substrates (2–10 μm groove width), inducing over 80% cell alignment along the principal axis.[21,48–50] Similarly, substrate stiffness can be tuned from 0.5 kPa (brain-like) to 50 kPa (pre-calcified bone) using polyacrylamide or PEG-based hydrogels, directly modulating YAP/TAZ nuclear localization and contractility.[9]

Beyond structural support, the ECM regulates cell signaling through sequestered growth factors or cytokines, mechanotransduction pathways (the conversion of mechanical signals to biochemical responses), and dynamic remodeling mediated by enzymes such as lysyl oxidase and MMPs.[31,46,51] In 4D tissue engineering, growth factor presentation is engineered via heparin-mimetic domains or MMP-degradable cross-linkers (e.g., VPMSMRGG peptide sequences), enabling on-demand release of vascular endothelial growth factor (VEGF) or transforming growth factor (TGF)-β1, with a release half-life of 3–14 days.[52] Acting as a modulator of cell–ECM adhesion, growth factor availability, and chemotactic (chemokine gradients)/haptotactic (directional migration) guidance cues, the ECM orchestrates differentiation, maturation, and directed migration of both resident and recruited cells.[47,51,53]

Serving as a non-cellular, 3D scaffold, the ECM integrates mechanical and biochemical cues to regulate cell fate. Its biophysical properties arise from four core classes of macromolecules that directly inform biomaterial design: structural proteins, elastic fibers, adhesive proteins, and amorphous proteoglycans (Figure 2).[54,55] These native components are increasingly preserved in dECM derived from tissues or organs, which retains organ-specific architecture, ligand presentation, and mechanical gradients. When combined with 3D or 4D bioprinting, dECM provides a direct, customized template that translates complex biophysical hierarchies into programmable, evolving scaffolds.[56,57]

Among the ECM's molecular constituents, structural proteins—including fibrillar collagens (types I–III, V; hydrated Young's modulus of 0.5–100 kPa), network-forming collagen IV (approximately 400 nm wire sheets, 10–50 kPa), fibril-associated collagen VI (beaded microfilaments), elastin (entropic recoil, 0.1–1.5 MPa), and fibrillin-rich microfibrils—constitute the hierarchical, load-bearing backbone that generates anisotropic stiffness gradients, pronounced strain-stiffening, and viscoelastic dissipation (Figure 2A and B).[54,58] Secreted by fibroblasts, chondrocytes, and osteoblasts, collagens self-assemble into fibrils, primarily influenced by hydrophobic and electrostatic interactions between collagen molecules; the resulting fibrillar architecture influences cell polarity and supports morphogenesis. In contrast, elastin governs tissue elastic modulus for recoil while guiding cell alignment and differentiation via integrin-mediated signaling.[59]

These native biophysical signatures are recapitulated in engineered scaffolds through 200 nm electrospun fibers (produced via rotating mandrels or parallel electrodes) for contact guidance and durotaxis, tunable cross-linking density with genipin (0.05–0.5 wt%) or ruthenium/sodium persulfate photo-cross-linking to replicate physiological strain-stiffening and relaxation timescales, and incorporation of recombinant tropoelastin or elastin-like polypeptides for recoverable entropic elasticity.[49,60,61]

Nevertheless, current structural protein-derived and protein-informed materials still fall short of native fatigue resistance (>10^7 cycles at 10–20% strain), long-term *in vivo* stability (elastin half-life >70 years versus months-to-years for most constructs), batch-to-batch reproducibility, and regulatory approval due to residual cross-linker toxicity and telopeptide immunogenicity.[62,63] In 4D tissue engineering, these deficiencies have become critical bottlenecks, as the materials typically lack the robust creep resistance and reversible viscoelasticity needed to sustain programmed, time-evolving shape changes and adaptive remodeling under decades-long physiological loading, resulting in premature loss of dynamic function well before full tissue maturation.[63] This has led to commercial collagen gels often being blended with synthetic polymers like PEG to improve long-term stability.[64]

While structural proteins provide mechanical robustness, adhesive proteins (e.g., fibronectin, laminin, and thrombospondins [TSPs]) act as molecular bridges between cells and the ECM by presenting integrin-binding domains (e.g., RGD, IKVAV, YIGSR) at precise densities and nanometer-scale spacings (optimal 10–150 nm; Figure 2C).[54] These parameters directly control focal

adhesion maturation, cytoskeletal tension, and downstream cell polarity, thereby dictating the required grafting chemistry, peptide concentration (0.1–10 mM), and patterning method (microcontact printing, nanopatterned surfaces) for material design.[65,66]

Fibronectin is a mechanosensitive glycoprotein that serves as a master organizer of the ECM, enabling integrin-mediated cell adhesion, fibril assembly, and exposure of cryptic binding sites under mechanical load to regulate matrix remodeling, stability, and downstream focal adhesion kinase/extracellular signal-regulated kinase signaling, which are critical for polarization, collective migration, morphogenesis, and gastrulation.[67,68] In 4D tissue engineering, precise spatial presentation of its RGD and PHSRN synergy sites at 10–70 nm spacing is essential to trigger maturation of focal adhesions, generate cytoskeletal tension, and drive time-dependent cell polarity and shape changes in dynamic matrices.[55,69–71] Current examples include adsorbed full fibronectin or linear/cyclic RGD-grafted PEG, HA, or polyacrylamide hydrogels and poly(lactic-co-glycolic acid) (PLGA) scaffolds, which significantly improve initial cell attachment and viability.[4,72,73] However, adsorbed protein may denature or orient randomly, xenogeneic sources show batch variability, and short linear RGD peptides exhibit 100–1000-fold lower affinity than native fibronectin, requiring non-physiological densities that fail to recapitulate synergy-dependent mechanotransduction or maintain long-term stemness.[74]

Laminin, the primary adhesive glycoprotein of basement membranes, provides essential IKVAV, YIGSR, and isoform-specific RGD motifs that direct cell polarization, axon guidance, epithelial, muscular, or vascular differentiation, and tissue barrier formation through integrin and dystroglycan binding and synergistic interactions with collagen type IV and nidogen (Figure 2C).[47,54,59,75] In polarized tissue engineering (e.g., vessels, neural tubes, kidney organoids), 4D systems require precise nanoscale clustering and orientation of adhesive peptides to drive apico-basal polarity and sustained lineage commitment within stimuli-responsive matrices.[55,75] Currently, laminin-derived materials such as Matrigel, Cultrex, or Geltrex, laminin-111/521 coatings, and PEG/HA hydrogels functionalized with IKVAV or YIGSR, have been observed to promote vascularization and neural regeneration in preclinical models.[76–78] However, tumor-derived Matrigel has an undefined composition, high batch variability, residual mitogens, and tumorigenic risk.[79] Similarly, purified full-length laminin remains prohibitively expensive and unstable. At the same time, short peptides mimic its activity only partially and show markedly weaker polarization, axon extension, and organoid morphogenesis compared to the native protein.[80]

In addition, TSPs are context-dependent matricellular proteins. TSP-5, also known as cartilage oligomeric matrix protein (COMP), and TSP-1–4 modulate angiogenesis, inflammation, collagen fibrillogenesis, and mechanotransduction via RGD (TSP-1/2), cysteine–serine–valine–threonine–cysteine–glycine (TSP-1), and valine–valine–methionine (TSP-5) motifs, with TSP-1/2 typically anti-angiogenic through VEGF sequestration and TGF-β activation, whereas TSP-5/COMP supports high-load tissue assembly in cartilage and tendons (Figure 2D).[81–83] Their mechano-responsive incorporation enables time-controlled switching between pro- and anti-angiogenic states and stiffness reinforcement during load-bearing tissue maturation. Current applications include COMP-supplemented collagen scaffolds for tendon/ligament repair and TSP-1/2 peptide-doped fibrin or collagen gels to fine-tune vascular ingrowth.[83–85] However, limitations remain significant due to high context- and concentration-dependence (excess TSP-1/2 strongly inhibits vascularization and delays healing),[86] often resulting in the uneven incorporation and rapid *in vivo* degradation of multimeric proteins, restricting predictable 4D control over angiogenesis and mechanical evolution.

Beyond structural and adhesive proteins, proteoglycans and their GAG chains—HA, HS, and chondroitin/dermatan sulfate (CS/DS)—are primary regulators of ECM hydration, compressive resistance, viscoelasticity, and morphogen presentation. Their high negative charge density generates substantial osmotic swelling pressures (200–1000% volume increase), while specific binding pockets for fibroblast growth factors (FGFs), VEGF, bone morphogenetic proteins (BMPs), and TGF-β establish gradients, amplify signaling, and protect growth factors from degradation. Together, these functions modulate collagen assembly and mechanotransduction across cartilage, basement membranes, and other load-bearing tissues (Figure 2E and F).[55,87–90] These gradients are essential for processes such as angiogenesis, chondrogenesis, and neural development. For example, perlecan facilitates BMP-2 signaling and TGF-β activity during bone formation, and aggrecan supports cartilage zonal organization.[76,90,91]

Proteoglycans are used in tissue engineering for their extreme swelling capacity, shear-thinning injectability, enzyme-triggered degradability (hyaluronidase, heparanase, chondroitinase), and growth-factor sequestration/release kinetics,[88,90] thereby promoting highly dynamic, cell-mediated remodeling systems that evolve stiffness, porosity, and bioactive gradients over time for vascularization, chondrogenesis, organoid patterning,

and load-adaptive maturation.[56,90] Nevertheless, substantial limitations remain due to native GAG sulfation patterns and molecular weight-dependent bioactivities being nearly impossible to replicate synthetically, and animal-derived GAGs exhibiting batch variability and immunogenicity.[92]

Extending beyond classical ECM molecules, growth factors (e.g., VEGF, FGF, platelet-derived growth factor, BMPs, TGF-β), cytokines (e.g., interleukin-6, tumor necrosis factor α, interferons), and cell–cell adhesion molecules (e.g., cadherins, selectins, connexins, and non-RGD-binding integrin heterodimers) collectively orchestrate proliferation, migration, differentiation, inflammation, immune cell trafficking, junction formation, and tissue-level morphogenesis through highly transient, gradient-dependent, and switchable signaling that classical ECM proteins alone cannot provide.[54,93] These molecules enable temporal control of signaling via affinity-regulated, enzyme-, plasmin-, light-, or shear-triggered release systems, dynamic morphogen gradients, reversible cell

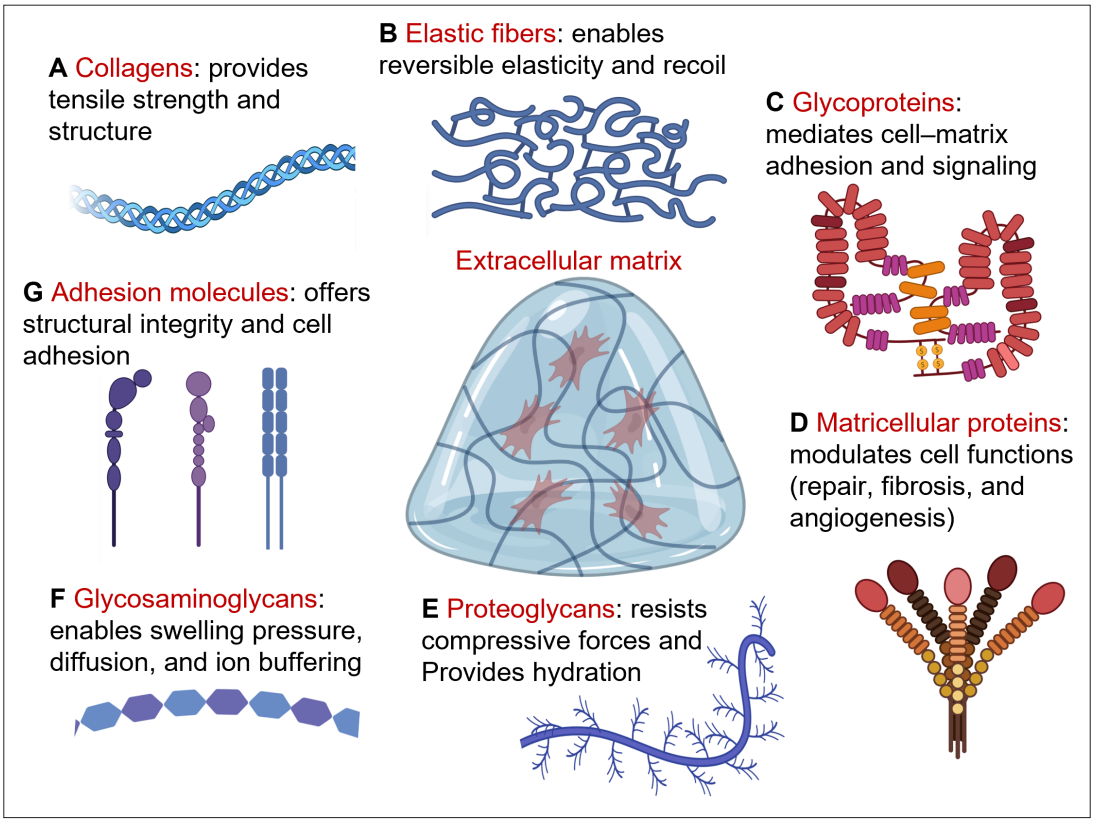

Figure 2. Key extracellular matrix (ECM) components and their functional roles. (A) Collagens (fibrillar collagens types I–III and V; network-forming collagen type IV): Providing tensile strength and structural scaffolding in ECMs, forming fibrils (types I–III and V) for resistance to traction and networks (type IV) in basement membranes for tissue organization. (B) Elastic fibers (e.g., elastin, microfibrils): Permitting reversible elasticity and recoil to tissues such as arteries, lungs, and skin, enabling repetitive deformation. Elastin provides long-range extensibility via cross-linked tropoelastin, while microfibrils (fibrillins) act as scaffolds. (C) Glycoproteins (e.g., laminins, fibronectin, thrombospondins): Mediating cell–matrix adhesion and signaling. Laminins form basement membrane networks for tissue morphogenesis, cell differentiation, migration, and homeostasis. Fibronectin organizes ECM assembly, promotes cell adhesion via integrins, and regulates migration, proliferation, and wound healing. (D) Matricellular proteins (e.g., thrombospondins (TSP)-5/cartilage oligomeric matrix protein and TSP 1–4): Temporarily modulate cell functions without structural roles. TSP-5/cartilage oligomeric matrix protein regulates cartilage organization, collagen fibrillogenesis, and chondrocyte proliferation. TSP 1–4 control angiogenesis, fibrosis, wound healing, and cell–matrix interactions, with anti-angiogenic and pro-fibrotic activities in disease contexts. (E) Proteoglycans (e.g., aggrecan, versican, brevican): Provide hydration, compression resistance, and signaling modulation. Aggrecan aggregates with hyaluronan in cartilage for shock absorption. Versican regulates cell motility, proliferation, and tissue morphogenesis. Brevican supports neuronal adhesion and the formation of the brain ECM. (F) Glycosaminoglycans (e.g., chondroitin sulfate, heparan sulfate, heparin, and hyaluronic acid): Provide hydration, create negative charge, and space-filling properties. Chondroitin sulfate enables swelling and compression resistance. Heparan sulfate/heparin binds growth factors for signaling and angiogenesis. Hyaluronic acid maintains tissue hydration, facilitates cell migration, and regulates inflammation and wound healing. (G) Adhesion molecules (e.g., cadherins, selectins, connexins): Facilitate cell–cell and cell–matrix interactions. Cadherins mediate calcium-dependent cell adhesion to maintain tissue integrity and support morphogenesis. Selectins enable leukocyte rolling and adhesion during inflammation. Connexins form gap junctions for intercellular communication and signaling in tissues like the heart and the nervous system. Created in BioRender. Joung, D. (2025). https://BioRender.com/hbg6tqr.

clustering, epithelial–mesenchymal transitions, and inflammation-to-resolution switching, all essential for vascular sprouting, organoid self-organization, immune-evasive implants, and tissue fusion.[55,93]

Current platforms include heparin/star-shaped PEG (starPEG) or MMP-degradable PEG hydrogels for sustained/sequential VEGF–platelet-derived growth factor–BMP-2 delivery in bone and vascular models, and cadherin-11 or N-cadherin peptide-functionalized modular HA/PEG assemblies for cardiac and neural spheroid fusion.[94,95] Even so, cadherin/connexin peptides achieve only 1–10% of native affinity and cannot replicate inside-out signaling or catch bonds.[96] Above all, the lack of true ON/OFF switchable systems forces 4D constructs into irreversible, one-time-release approaches, failing to mimic the oscillatory, feedback-regulated signaling of native development and healing.[97]

Together, these ECM and microenvironmental components form a spatiotemporally orchestrated system that cohesively regulates tissue mechanics, hydration, adhesion, polarity, morphogen gradients, inflammation, and remodeling via nanoscale ligand display, force-dependent unfolding, enzyme-triggered release, and feedback signaling. These elements directly guide 4D SMART biomaterial design by providing blueprints for dynamic stiffness evolution, on-demand ligand clustering, switchable growth-factor gradients, reversible cell polarity, inflammation resolution, and load-adaptive remodeling, thereby converting static scaffolds into regenerative microenvironments that drive vascularization, organoid patterning, zonal maturation, and host integration.

Current platforms integrate multi-domain peptides, injectable GAG hydrogels, heparin/HS affinity modules, MMP-degradable linkers, and cadherin/RGD assemblies to mimic physiological dynamics in bone, cartilage, vascular, neural, and cardiac models. However, clinical translation is constrained by incomplete replication of native complexity (e.g., sulfation codes, synergy sites, catch bonds, oscillatory signaling), batch variability and immunogenicity of biological sources, loss of responsiveness from over-stabilization, and the absence of truly reversible, multi-modal triggers. Synthetic ECMs, therefore, remain partial mimics of natural developmental and homeostatic fidelity. Table 1 summarizes the functions of major ECM and microenvironment components used in 4D SMART materials, as described above.

2.2. Tissue-specific extracellular matrix compositions

Now that we have explored the ECM components, the next step is to examine how their integration at varying

Table 1. Extracellular matrix and microenvironment components and their roles in 4D SMART materials

Component	Role in 4D SMART materials	Materials available	Ref.
Collagens	Enables tunable stiffness and degradation	Collagen gels, collagen–polyethylene glycol bioinks, electrospun nanofibers.	15,48,55
Elastin	Provides elasticity and recoil for dynamic tissues	Tropoelastin hydrogels, ELP additives	98–101
Elastic microfibrils	Enables tension-responsive unfolding and growth factor release	Fibrillin composites, microfibril-GelMA	55,70
Fibronectin	Improves adhesion and signaling via RGD	Fibronectin-based hybrids, PNIPAAm gels	102–105
Laminin	Supports BM formation and cell polarity	Laminin-enriched, laminin peptide-hybrids	77,106,107
Glycoproteins/TSPs	Modulate angiogenesis, stabilize cartilage, and control growth factor release	TSP-based hybrids, glycoprotein additives.	85
Proteoglycans	Provide hydration and growth factor reservoirs	Aggrecan–HA, perlecan–HS, syndecan–polyethylene glycol scaffolds	108–110
Glycosaminoglycans	Enable turgor-based shape changes and bind growth factors for controlled release	HA hydrogels, heparin-functionalized gels	73,99
Growth factors	Drive cell differentiation and patterning	VEGF, EGF, FGF-2, BMP-2, TGF-β	109,111–113
Cytokines	Modulate inflammation and tissue integration	IL-4, G-CSF, SDF-1α	114,115
Adhesion molecules	Enhance force-responsive adhesion and self-organization	RGD/LDV-polymers, cadherin/integrin/selectin-additives	72,116,117

Abbreviations: 4D: four-dimensional; BM: basement membrane; BMP: bone morphogenetic protein; EGF: epidermal growth factor; ELP: elastin-like polypeptide; FGF: fibroblast growth factor; G-CSF: granulocyte colony-stimulating factor; GelMA: gelatin methacryloyl; HA: hyaluronic acid; HS: heparan sulfate; IL: interleukin; LDV: leucine–aspartic acid–valine; SDF-1α: stromal cell–derived factor 1α; SMART: stimuli-responsive materials for advanced regenerative technologies; RGD: arginine–glycine–aspartic acid; TGF: transforming growth factor; TSP: thrombospondin; PNIPAAm: poly(N-isopropylacrylamide); VEGF: vascular endothelial growth factor.

ratios generates tissue-specific functionality—ultimately informing future experimental design. Tissue-specific ECM compositions emerge from organ-unique ratios and spatiotemporal assembly of structural proteins (e.g., collagen types I–V, elastin), adhesive glycoproteins (e.g., fibronectin, laminin, TSPs), amorphous proteoglycans/GAGs (e.g., HA, HS, CS/DS), and transient cues (e.g., growth factors, cytokines, cadherins), yielding either collagen/proteoglycan-dominant interstitial matrices for load-bearing tissues (e.g., cartilage, bone, tendon, dermis) or laminin/collagen type IV/perlecan-rich basement membranes for polarized tissues (e.g., epithelium, endothelium, neural).[26] These signatures define organ-specific mechanics (0.1–1000 kPa), viscoelasticity, ligand spacing, hydration, and morphogen kinetics, serving as the foundational template for 4D SMART biomaterials.

Successful clinical application requires precise replication of these ratios using translatable modules (e.g., Matrigel, Cultrex, HAMA, starPEG–heparin, recombinant collagens, RGD/cadherin peptides) combined with degradable linkers and affinity systems. This would enable authentic dynamic evolution of stiffness, ligand presentation, gradients, and remodeling, thereby driving proper lineage commitment, polarity, vascularization, and zonal maturation while preventing fibrosis or aberrant differentiation from generic matrices.

Starting with general epithelial tissues, these tissues primarily possess a thin, basement membrane-dominated ECM with characteristic compositional ratios (collagen type IV: ~30–40%, laminins: ~10–15%, HS proteoglycans [e.g., perlecan]: ~5–10%, minor interstitial collagens type I/III: ~20–25%, fibronectin: ~10–15%, and HA: ~5–10% for hydration), which set low initial stiffness (0.1–5 kPa), strong apico-basal polarity cues, and selective permeability for nutrient/waste transport.[26,54,118] In polarized epithelia located in glands, intestines, or kidneys, these precise starting ratios must be faithfully reproduced in dynamic hydrogels to initiate authentic stem cell symmetry breaking, lumenogenesis, and barrier maturation.[119,120] Deviation from these tissue-specific ratios can disrupt lumen formation, invert polarity, or trigger unwanted epithelial–mesenchymal transition.[120,121]

Similar to general epithelia, skin ECM exhibits a hierarchical composition, with the dermal interstitial matrix dominated by collagens (~70–80%, primarily type I [~60–70%] and type III [~10–15%]), elastin (~2–5%), fibronectin (~5–10%), and proteoglycans such as decorin/biglycan (~5–10%), with chondroitin/dermatan sulfate-rich GAGs (~5–10%), capped by a thin epidermal basement membrane enriched in collagen type IV, laminin-332, and perlecan. This arrangement collectively establishes high tensile strength (10–100 kPa), viscoelastic recoil, rapid hydration/swelling, and layered polarity essential for barrier integrity, wound contraction, and sensory function.[54,122] This multi-layered matrix supports keratinocytes in the epidermis (basement membrane) and fibroblasts in the dermis, facilitating barrier function, providing elasticity and hydration, supporting wound healing (driven by fibronectin and HA), and serving sensory roles that the protective skin layer needs to continuously maintain.[26,76,122]

In contrast to the skin's compact matrix, lung ECM is distinctly compartmentalized into thin basement membranes and loose interstitial matrices, with defined compositional ratios (collagens: ~40–50%, primarily types I/III [~30–40%] and type IV [~10–15%]; elastin: ~15–20%; versican proteoglycans: ~20–25%; and heparan/chondroitin sulfate GAGs: ~10–15%) that collectively confer ultra-low stiffness (0.1–5 kPa), extreme viscoelastic recoil, and high hydration, supporting efficient gas diffusion, alveolar expansion, and lung compliance.[123–125] In 4D bioengineering of alveolar or bronchial constructs, these ratios can be recapitulated in ultra-soft, poroelastic hydrogels as an initial instructive template to drive authentic type I/II pneumocyte barrier formation, endothelial capillarization, and cyclic mechanical breathing-like actuation.[26,124,126,127] Additionally, abundant elastin and versican enable passive recoil and matrix swelling, ensuring ventilation fidelity, while tightly regulated collagen content limits premature fibrotic deposition yet permits stretch-induced remodeling. HS domains preserve VEGF/FGF gradients required for vascular parity, with subsequent MMP- and heparanase-triggered matrix evolution facilitating inflammation resolution and physiological stiffening only in response to injury cues.[124,126,128–130] Deviations from these compositional ratios trigger irreversible scarring, alveolar collapse, or stiff, non-compliant constructs, which likely underlie the widespread failure of generic matrices to produce functional, gas-exchanging lung organoids or regenerative implants.

Skeletal muscle ECM displays hierarchically organized compositional ratios (~5–10% collagen, primarily types IV/VI in the endomysium and I/III in the perimysium, together with decorin/biglycan proteoglycans, elastin, and heparan/chondroitin sulfate GAGs) that generate aligned anisotropy, viscoelastic compliance (0.1–10 MPa), and specialized pericellular niches supporting myofiber force transmission, contraction, and satellite cell-mediated repair.[46,131–133] This matrix forms a flexible pericellular network that anchors or aligns myofibers, facilitating force transmission, muscle contraction, and satellite cell-driven regeneration, thereby supporting functional mobility and tissue repair.[26,46,51,133] In bioprinting and tissue engineering of volumetric muscle constructs, these defined ratios

should be recapitulated in aligned fibrillar hydrogels as an instructive template to drive authentic myoblast fusion, sarcomerogenesis, and load-responsive maturation.[134] Collagen type IV/VI and HS-rich domains preserve early soft niches for satellite cell activation and migration. In contrast, collagen type I/III, elastin, and decorin enable subsequent stretch-induced fibril alignment and stiffening, supporting mature contractile bundle formation and vascular integration.[14,46,133,134]

Moving from soft to semi-rigid tissues, the cartilage ECM exemplifies a matrix specialized for compressive load bearing and hydration retention. Found in articulating surfaces, tracheal rings, and the embryonic skeleton, hyaline cartilage consists of collagen type II (~40–50%), aggrecan proteoglycans (~25–35%), GAGs (chondroitin and keratan sulfates; ~20–30%), and fibronectin (~5–10%).[26,54,135] The aggrecan–hyaluronan aggregates generate high osmotic swelling pressure, imparting viscoelastic resistance and smooth, low-friction surfaces essential for joint articulation.[135,136] These compositional principles have been leveraged in bioprinting and tissue-engineering approaches, where dECM scaffolds and stem cell-laden constructs recapitulate cartilage structure for osteoarthritis repair and joint resurfacing.[32,137] Deviations from these ratios have been shown to induce fibrous tissue formation, superficial delamination, or ectopic ossification.[99,136,138]

Building upon this progressive increase in rigidity, bone ECM is predominantly composed of collagen type I (~85–90%), with hydroxyapatite minerals (inorganic phase), biglycan/decorin proteoglycans (~1–5%), and GAGs such as chondroitin/dermatan sulfate (~1–5%).[54,139] This ratio confers extreme stiffness (100–200 MPa), fracture toughness, and nanostructured porosity through aligned mineralized fibrils, supporting compressive and tensile strength, impact absorption, and osteocyte mechanotransduction.[137,139–141] Accordingly, material composites such as calcium phosphate–collagen hydrogels, HA–PCL, and tricalcium phosphate–CS blends mimic the mineralized ECM for osteoporosis models, enhance load-bearing, and improve antimicrobial properties.[91,140–142]

Closely related yet functionally distinct, the ECM in cardiac muscle is a dynamic network primarily composed of collagen types I/III (~5–15%) and IV (~5–10%), syndecan-4 proteoglycans (~5–10%), elastin (~5–10%), and GAGs (~5–10%).[125,143] It serves as a reservoir for growth factors, cytokines, and proteases.[125] Structurally divided into the basement membrane/pericellular matrix (around cardiomyocytes, rich in laminin and collagen type IV) and the interstitial matrix (providing structural support via collagen type I/III), cardiac fibroblasts are the main producers of cardiac ECM, with contributions from endothelial cells and cardiomyocytes.[54,125,143] This organization yields a compliant scaffold for rhythmic function, cardiomyocyte adhesion, and electrical conduction, essential for heartbeat regulation.[144,145]

Soft, dynamic hydrogels serve as the optimal starting template to drive authentic human induced pluripotent stem cell–cardiomyocyte alignment, synchronous beating, and fibroblast co-maturation.[145] Elevated pericellular laminin, collagen type IV, and syndecan-4 preserve early compliant niches for calcium transient initiation, whereas controlled interstitial collagen type I/III and elastin enable cyclic strain amplification and elastic recoil, ultimately permitting cell-driven, lysyl oxidase-mediated matrix stiffening and VEGF gradient formation that yield vascularized, contractile cardiac tissue.[143]

Extending this structural hierarchy, vascular ECM in arteries is formed through a layered structure beginning with the tunica intima (an endothelial basement membrane rich in collagen type IV and laminin), tunica media (smooth muscle cells embedded in elastic lamellae of elastin and fibrillin), and tunica adventitia (rich in collagen types I and III, conferring tensile strength).[123,144] Generalized vascular ECM includes elastin (~20–30%), collagen types I/III (~30–40%) and IV (~10–15%), syndecan/perlecan proteoglycans (~10–15%), and GAGs like HS (~10–15%).[123,125,146] This matrix creates a distensible conduit for circulation, supports endothelial barrier function, anticoagulation, and hemodynamic adaptation, and promotes nutrient transport and inflammatory regulation.[123,144,147] Biomaterials used to emulate the biophysical dynamics of this tissue range from decellularized aorta hydrogels to composites that integrate elastin-like peptides with collagen or PCL, supporting vascular grafts and 3D vascular network formation in bioprinting constructs.[22,146,148–150] Disruptions of these vascular-specific ratios can result in thrombosis, intimal hyperplasia, or rupture.

Lastly, the central nervous system ECM, which occupies approximately 10–20% of brain volume, exhibits compositional ratios (aggrecan/brevican/neurocan proteoglycans ~20–30% with chondroitin sulfate GAGs ~20–30%, collagen type IV ~5–10%, and laminins ~10–15%) that form ultra-soft (0.1–1 kPa) diffuse perisynaptic gels and condensed perineuronal nets for neuroprotection against oxidative stress and excitotoxicity, while constraining molecular diffusion to enable synaptic stabilization, activity-dependent plasticity, and long-term potentiation.[151–156] Decellularized brain ECM coatings and scaffolds created with HA-dominant chondroitin sulfate proteoglycans-rich hydrogels enhance neuronal viability, neurite outgrowth, and network formation in neuron–glia co-cultures.[157] Failure to preserve these neural-specific

ratios can lead to hyperexcitability, gliosis, or failed synaptogenesis.

Taken together, these examples illustrate how tissue-specific ECM composition and architecture dictate distinct mechanical, biochemical, and signaling landscapes across organ systems. Understanding these nuances provides the foundation for designing 4D SMART materials that can dynamically replicate, remodel, and respond to native tissue microenvironments—bridging the gap between static biomaterials and living, adaptive tissue constructs.

3. 4D SMART materials

3.1. Applications of stimuli-responsive materials

Characterized by their stimuli-responsive adaptivity, SMART materials build off first-generation ECM-mimicked biomaterials which provide baseline localized biochemical and biophysical cues to influence cell behavior, and advance toward a next-generation transformative class of biomaterials that evolve over time in response to external triggers such as temperature, humidity, pH, light, or magnetic fields, thereby enabling dynamic shape-shifting, self-assembly, and conformational changes akin to living systems (Table 2).[12,22,76,158]

Specifically engineered to mimic key properties of the ECM, many current materials are multi-adaptive, integrating two or more response mechanisms to support cell encapsulation and enable stimuli-triggered behaviors, such as self-folding in 4D bioprinting.[18,91,145] Replicating the biophysical dynamics of the ECM introduces inherent biomaterial toxicity risks, typically arising from material composition (e.g., residual monomers, oxidative groups), dose/concentration, exposure duration, and processing conditions (e.g., crosslinking agents), thereby affecting cell viability. Cell viability is further influenced by material biocompatibility, porosity, stiffness, and nutrient and reagent diffusion capacity, and is often assessed via assays such as the 3-(4,5-dimethylthiazol-2-yl)-2,5-diphenyltetrazolium bromide (MTT) assay (metabolic activity) and live/dead staining.[3,159,160] With this context, we next organize SMART materials by primary stimulus class and highlight representative systems, followed by multi-trigger integrations that exemplify 4D behavior.

3.1.1. Thermo-responsive polymers for four-dimensional actuation and tissue engineering

Thermo-responsive (temperature-sensitive) materials are primarily found as polymers, such as PNIPAAm, PNIPAAm derivatives, or Pluronic, which undergo reversible physicochemical changes in response to temperature shifts.[184,185] These materials mimic the temperature-driven conformational shifts of collagen and elastin during wound healing and development, enabling printed constructs to soften or stiffen in situ, mimicking maturing tissues.[5] These polymers are classified into two types: lower critical solution temperature (LCST) and upper critical solution temperature (UCST).[5,186] LCST types involve a phase transition (~32–34°C) in which, below LCST, solubility is maintained through hydrogen bonding with water, and above LCST, intramolecular hydrophobic collapse results in dehydration, gelation, or aggregation.[6,184] In UCST polymers (sulfobetaine-based), activation below UCST causes insolubility through strong hydrogen bonding or ion pairing, and above UCST, dissolution is promoted by thermal energy, hydrogen bonding, or electrostatic disruption.[5,6,184,187]

These polymers have been used in tissue engineering to facilitate cell sheet harvesting, where cooling triggers hydrophilic swelling, detaching intact cell sheets without enzymes, and preserving cell junctions for layered tissues such as the cornea or myocardium.[5,145,188] While PNIPAAm is praised for enabling enzyme-free cell harvesting in

Table 2. Activation of stimuli-responsive materials for advanced regenerative technologies

Stimulus type	Mechanism of activation	Ref.
Temperature	Triggers phase transitions in polymers, leading to shape recovery or transformation	161–166
pH	Triggers protonation/deprotonation in polymers, causing swelling/shrinking and shape changes in acidic or basic environments	164,167,168
Hydration	Induces swelling or deswelling in hydrophilic polymer networks, leading to volume expansion, shape deformation, or actuation	164,169–171
Light	Photothermal, photochemical, or photoisomerization processes (NIR, IR, UV), enabling localized deformation, recovery, or actuation	162,168,172–174
Ionic strength	Crosslinking or gelation enabling shape fixation, actuation, or stiffness changes	175–177
Magnetic	External B-field, inducing actuation, alignment, or deformation	178–180
Electrical	External E-field, generating bending, contraction, or expansion	25,181–183

Abbreviations: NIR: near-infrared; IR: infrared; UV: ultraviolet.

cell sheet engineering and preserving cell junctions, its biocompatibility has been a key limitation, with issues including delayed re-solubilization upon cooling, potential cytotoxicity from monomers (*N*-isopropylacrylamide), and inflammatory responses *in vivo* at higher concentrations.[184] Generally, thermo-responsive hydrogels (e.g., PNIPAAm, PNIPAAm derivatives, Pluronic) are biocompatible with minimal effects on cell viability in short-term studies; however, long-term cytotoxicity and material degradation need to be further evaluated.[5,184,185]

3.1.2. pH-responsive polymers for four-dimensional dynamic biomaterials

pH-responsive materials, such as polymers and peptides, undergo reversible physicochemical transitions triggered by anionic interactions, which swell above a pKa via deprotonation (e.g., carboxylic acids), and cationic interactions, which swell below a pKa through protonation (e.g., amines).[189,190] These materials replicate the charge-dependent swelling and matrix remodeling observed in acidic inflammatory or tumor microenvironments, enabling localized volume changes akin to ECM acidification-driven fibrosis.[191]

Anionic polymers, such as poly(acrylic acid) or carboxymethyl cellulose (CMC), activate through deprotonation. When responses exceed the pKa thresholds, COO^- groups repel one another, leading to chain expansion and swelling. Conversely, below these thresholds, protonation neutralizes charges, leading to collapse.[189,190] Cationic polymers, such as chitosan (CS), protonate below pKa thresholds, where NH_3^+ repulsion induces swelling, while deprotonation above pKa thresholds promotes contraction.[189,191–193] CS is commonly used in dual-responsive bilayers, such as CS/CMC, which exhibit bidirectional actuation. CS swells at acidic pH due to NH_3^+ formation, whereas CMC swells at basic pH via COO^- ionization, with a structural equilibrium at neutral pH.[167] Mimicking pH shifts that occur during wound healing (inflammation), pH-responsive materials have been shown to facilitate the development of various programmable dynamic scaffolds and drug delivery systems.[189,190,194] These materials are generally considered biocompatible, and their toxicity and impact on cell viability depend on factors such as concentration, molecular weight, degree of modification, exposure duration, and pH.[189,190]

High doses or prolonged exposure can lead to cytotoxicity through mechanisms such as membrane disruption, oxidative stress, or apoptosis, and toxicity may vary as the material's conformation changes.[167,195] In recent studies, poly(acrylic acid) exhibits low to moderate cytotoxicity at typical biomedical concentrations, CMC shows excellent cell viability (>90%) at concentrations up to 5 mg/mL, and CS nanoparticles show dose-dependent toxicity, with >80% viability in lung carcinoma (A549) cells at <0.006% w/v, but <50% at higher doses due to reactive oxygen species (ROS) and membrane damage.[192,195–198]

3.1.3. Hydration-responsive materials for four-dimensional morphing scaffolds

Hydration-responsive, water-responsive, or humidity-sensitive materials (e.g., hydrogels, silk-based fibers, cellulose nanofibrils [CNF]) have been designed to mimic biological systems, where water plays a pivotal role in structural dynamics, and undergo reversible physical changes such as swelling, contraction, folding, or shape transformation through osmotic forces, molecular interactions with water, or changes in environmental relative humidity.[169,199,200] These behaviors are often observed in cartilage hydration during joint loading or in the maintenance of corneal transparency, enabling printed constructs to autonomously adjust stiffness and nutrient permeability in aqueous physiological environments.[201] These materials have been shown to be among the most biocompatible due to their organic sourcing, with more than 80% viability in alginate/HA scaffolding, 85–95% in CS/silk fibroin, and more than 90% in CNF composites.[196,197,202,203]

Integrating hydration- and thermo-responsive properties, Liu *et al.*[161] designed an amphiphilic dynamic thermoset polyurethane (DTPU) material for 4D printing to enable scaffolds with multidimensional morphing capabilities (1D–3D) for minimally invasive implantation, as shown in Figure 3A. These dual-responsive materials replicate the coupled moisture- and temperature-dependent viscoelasticity of articular cartilage and skin dermis, where combined humidity absorption and body-heat triggers produce synergistic softening or stiffening that mimics diurnal tissue compliance changes and thermoregulatory matrix remodeling.[204] DTPU—composed of PCL-triol as a thermo-responsive soft segment, PEG for hydrophilicity modulation, isophorone diisocyanate for pre-polymerization, and Diels–Alder (DA)-diol as a dynamic chain extender—forms a covalently crosslinked network with thermally reversible DA bonds, allowing extrusion-based fused deposition modeling printing at high temperatures.[161] Scaffolds were shown to exhibit body-temperature–triggered shape memory for initial recovery (1D–2D), which relies on PCL-triol's low melting point, enabling reversible transitions between glassy and rubbery states (Figure 3B).[161]

Followed by programmable deformation (2D–3D) through water absorption at 37°C, swelling induces a mismatch in bilayer structures, where high-swelling layers (DTPU-0.5-4k, swelling ratio: 118.1%) expand more than low-swelling ones (DTPU-0.25-4k, swelling ratio: 41.3%),

thereby generating internal stress for bending/folding into 3D shapes within 10 minutes (Figure 3C).[161] Stiffening also occurs in variants of PEG (molecular weight ≥2000), where hydration drives microphase separation, causing hydrophilic PEG aggregates to separate from hydrophobic PCL/DA segments, forming domains that increase the Young's modulus (*E*) up to 2.9-fold (0.7 MPa [dry] to 2.0 MPa [hydrated]; Figure 3D).[161] DTPU showed low toxicity, consistent with its PCL/PEG-based composition, with reported cell viabilities >90%.[4] Initial mild inflammation (cell infiltration) occurred at week 1, which eventually resolved by weeks 2–4 with tissue integration, with no significant toxicity or viability reduction *in vitro*.[161]

3.1.4. Photoactive polymers and nanomaterials in four-dimensional bioprinting

Light or photo-responsive (near-infrared [NIR], infrared [IR], ultraviolet [UV]) materials encompass polymers, peptides, and nanomaterials that undergo reversible or irreversible physicochemical changes upon exposure, enabling precise spatiotemporal control.[174,205–207] These systems emulate light-regulated cellular processes (e.g., phytochrome-like signaling in plants or UV-induced dermal remodeling), thereby providing precise, on-demand control over local stiffness and topography that mimics scar formation or angiogenic sprouting.[208] These materials are commonly observed as GelMA hydrogels, azobenzene-based polymers/peptides, carbon nanomaterials, and other functionalized nanoparticles.[148,205,207,209] Activation wavelengths are used to classify these materials. UV is used for high-energy reactions, where activation is enabled via photoisomerization (azobenzene trans-cis switching, altering hydrophobicity for self-assembly) or photocleavage (o-nitrobenzyl esters uncaging RGD peptides, exposing adhesive sites).[174,205,210,211] UV activation is associated with higher toxicity due to its high energy, limited tissue penetration, and potential to cause DNA damage or ROS production in the cellular environment.[209,210,212]

However, viability assays (e.g., MTT) have shown more than 80% cell survival for short exposures, whereas prolonged UV exposure can disrupt the cytoskeleton and reduce viability by 20–30%.[174] NIR/IR mechanisms involve up-conversion, triggering downstream reactions such as bond cleavage or photothermal heating, which converts light into heat via absorbers such as carbon nanotubes, causing hyperthermia for shape-memory transitions, drug/growth factor release, or cell modulation.[173,205,206,211] Due to overlapping thermal effects, NIR and IR are considered the safest options, with lower phototoxicity and deeper tissue penetration than UV or visible light.[205] Research shows that viability decreases by <20%, and neuronal cell viability remains >85% post-NIR exposure.[173,205,206,211]

Photo-responsive SMART materials have also been used to recapitulate angiogenesis by inducing growth factor release. For example, Meng *et al.*[213] engineered photothermal-responsive microcapsules composed of a GelMA core loaded with epidermal growth factor (EGF) or VEGF, encased within a PLGA shell functionalized with gold nanorods.[113,214] Upon NIR laser irradiation, localized heating ruptured the shell without compromising cell viability (>93% post-irradiation) or molecular functionality (Figure 4A).[213] Sequential activation every two days generated sustained VEGF gradients over a two-week period—mirroring physiological timescales of proliferation, migration, and angiogenic sprouting. This system overcame limitations of conventional 2D cultures and static 3D models by combining precise spatial organization of tumor cells, stromal fibroblasts, and endothelial cells with dynamic chemical signaling through programmable growth-factor release (Figure 4B). Using A549 lung carcinoma and M4A4 melanoma cells, they recapitulated key stages of metastatic progression—including tumor-driven VEGF secretion, endothelial activation, vessel sprouting, intravasation, and angiogenic expansion—closely mimicking how solid tumors stimulate neovascularization under hypoxic stress (Figure 4C–G). Collectively, these case studies demonstrate how light-responsive SMART materials translate developmental physics—including cell division, folding, lumen formation, and vascularization—into programmable, time-evolving constructs that more faithfully reproduce the dynamic behaviors of living tissues.

3.1.5. Multi-stimuli–responsive and reconfigurable four-dimensional biomaterial assemblies

To exploit multiple cues simultaneously, researchers are building reconfigurable assemblies with photocontrolled adhesion layered atop pH- and thermal-responsive components. For example, by incorporating pH, light, and temperature responsivity, multi-design reconfigurable hydrogel assemblies have been fabricated using a photocontrolled metallopolymer adhesive composed of ruthenium-containing (P-Ru) and thioether-containing (P-S) polymers, where reversible gluing of individual hydrogel units is used to form four distinct constructs (Figure 5).[168] This approach directly translates the multifaceted, orthogonal remodeling of ECM observed in dynamic niches such as the wound bed or tumor stroma, where simultaneous acidification, local heating, and optical signaling (e.g., from inflammatory ROS or photothermal events) orchestrate sequential deswelling, stiffening, and topographical reconfiguration akin to scar maturation and angiogenic invasion fronts.[5,9,21,208] The adhesive forms strong bonds via metal–ligand

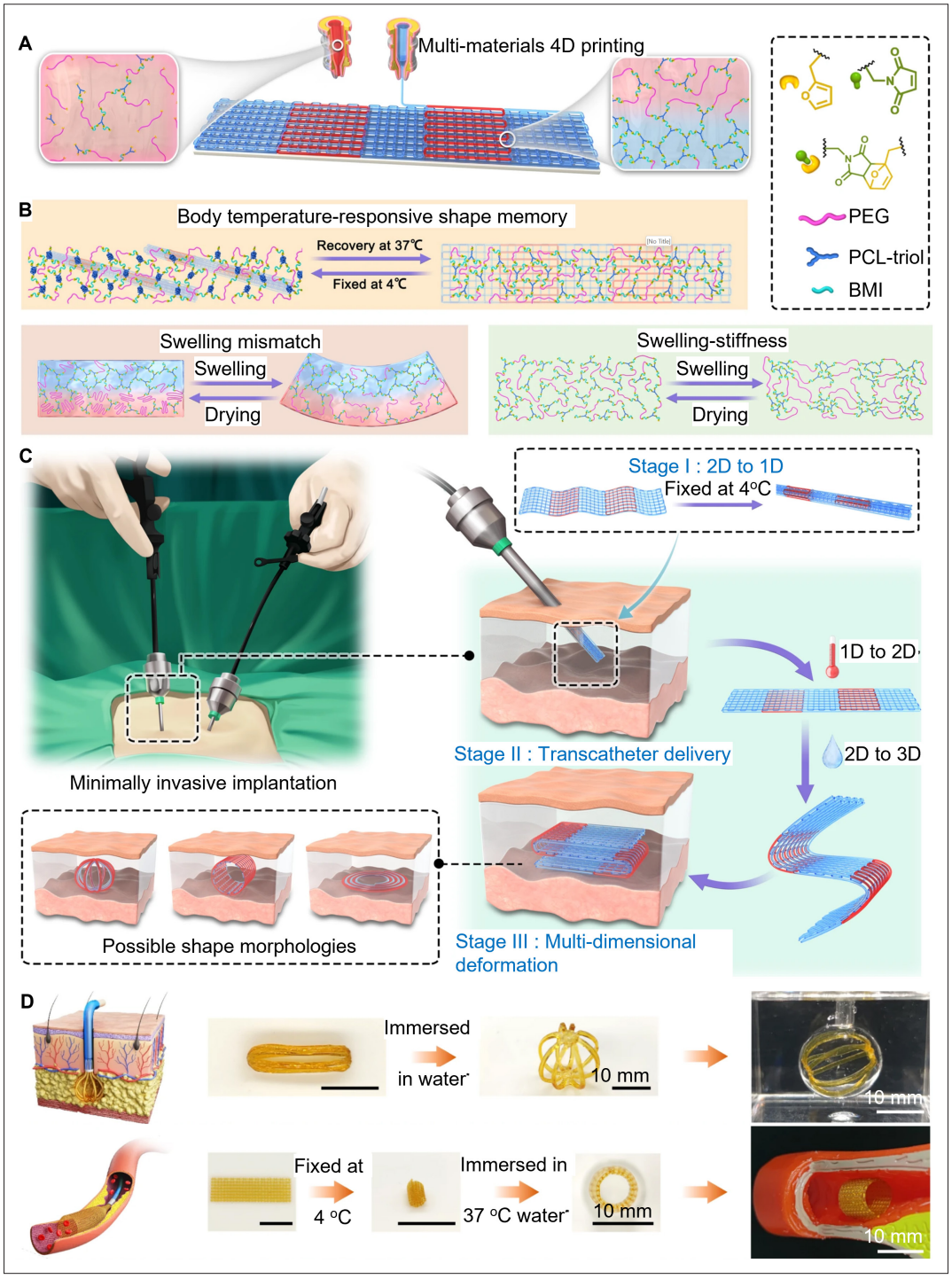

Figure 3. Hydration- and thermo-responsive stimuli-responsive materials for advanced regenerative technologies. (A) Fabrication of scaffolds via multi-material 4D printing, in which amphiphilic dynamic thermoset polyurethane is extruded through nozzles heated above the retro-Diels–Alder reaction threshold and layered onto a base to generate structures with differential swelling. (B) Fabricated scaffold demonstrating responsive shape memory activated by body temperature, with hydration-induced shape formation and increased rigidity upon water absorption. (C) Shape-shifting progression of the scaffold from 1D to 3D configurations in response to thermal and aqueous stimuli, enabling potential minimally invasive surgical deployment. (D) Diagrams and images of fabricated constructs illustrating multi-dimensional shape transformations, highlighting potential applications in soft tissue repair and vascular scaffolding. Shape changes are driven by water-activated programmable morphing and thermo-responsive recovery coupled with water-mediated reconfiguration. Adapted from Ref. [161] Abbreviations: 1D: one-dimensional; 2D: two-dimensional; 3D: three-dimensional; 4D: four-dimensional; BMI: bismaleimide; PCL: polycaprolactone; PEG: polyethylene glycol.

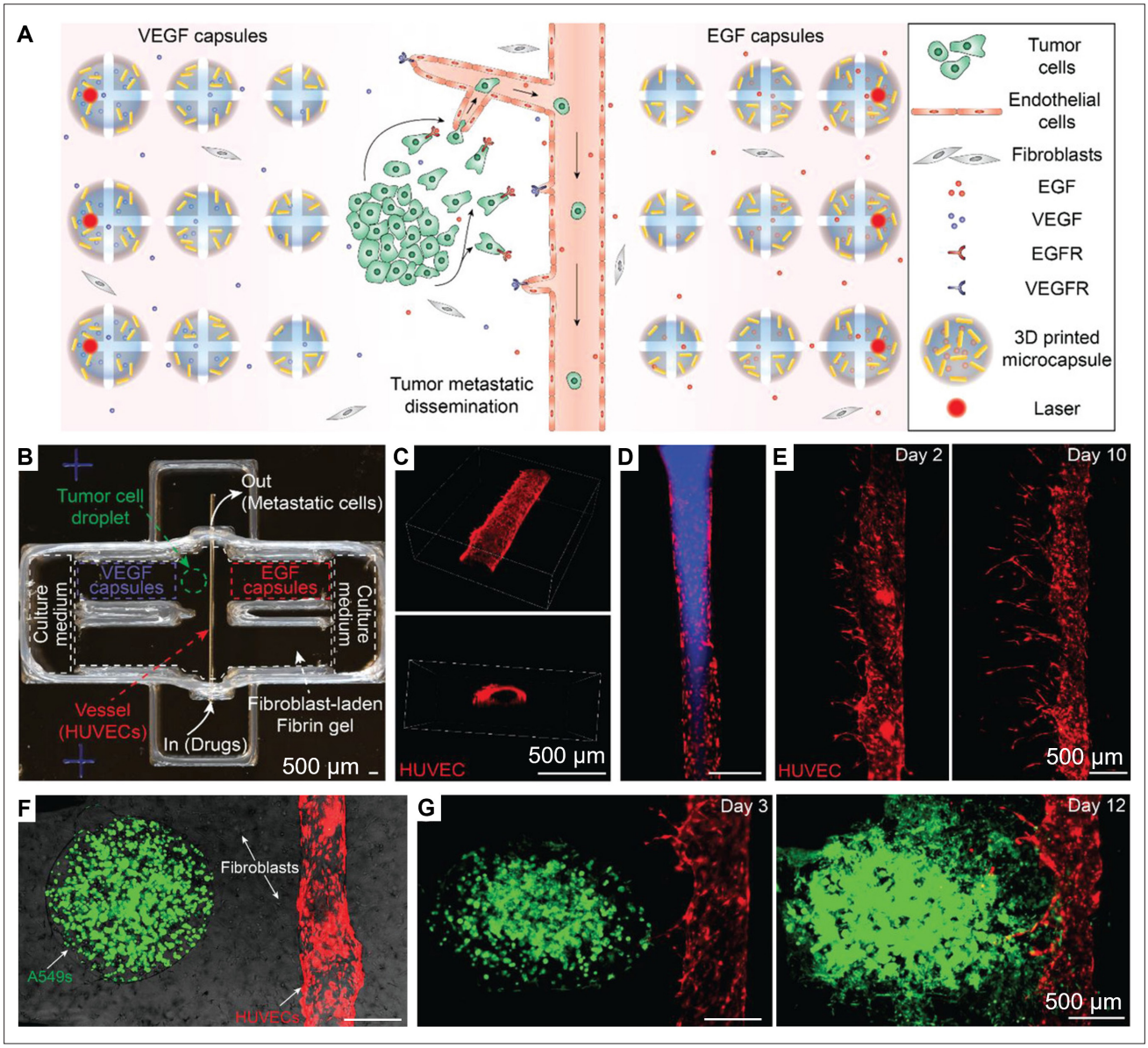

Figure 4. Tumor-induced neovascularization mimicking cancer metastasis. (A) Schematic of 3D bioprinted *in vitro* tumor models integrating tumor cells, endothelial-lined vascular conduits, and biochemical signals within a fibroblast-laden fibrin gel to recapitulate the tumor microenvironments. EGF and VEGF gradients are dynamically generated via programmable release capsules targeting EGFR and VEGFR. (B) Image of a 3D-printed culture chamber designed to guide tumor cell dissemination (scale bar: 500 μm). (C) Confocal images showing top (upper) and cross-sectional (lower) views of HUVEC-lined microchannels in fibrin gel, highlighting the vessel lumen (scale bar: 500 μm). (D) Fluorescence image of a vessel perfused with blue fluorescent fluid (derived from poly(fluorescein isothiocyanate allylamine hydrochloride)) (scale bar: 500 μm). (E) Panoramic fluorescence images showing directional vessel sprouts over time (days 2 and 10) guided by VEGF capsules (scale bar: 500 μm). (F) Composite image of a representative tumor model prior to laser-triggered EGF and VEGF capsule rupture (green: GFP-A549 cells; red: RFP-HUVECs; bright-field: fibroblasts) (scale bar: 500 μm). (G) Time-lapse fluorescence images (days 3 and 12) showing GFP-A549 tumor cells invading the fibroblast-laden fibrin gel and entering the vasculature (green: GFP-A549; red: RFP-HUVECs) (scale bar: 500 μm). Reprinted with permission from Ref. [213] Copyright © 2019, John Wiley & Sons. Abbreviations: 3D: three-dimensional; EGF: epidermal growth factor; EGFR: epidermal growth factor receptor; HUVEC: human umbilical vein endothelial cell; RFP: red fluorescent protein; VEGF: vascular endothelial growth factor; VEGFR: vascular endothelial growth factor receptor.

coordination and polymer chain entanglement, using blue light irradiation (470 nm) to trigger photochemical hydrolysis and dissociation of Ru-S to Ru-H_2O, thereby inducing a gel-to-liquid transition and detachment, as shown in Figure 5A. This enables constructs that respond to temperature and pH stimuli, where non-responsive P1 gels (cross-linked *N*-hydroxyethyl acrylamide) are combined with thermo-responsive P2 gels (zwitterionic 3-dimethyl[methacryloyloxyethyl] ammonium propane sulfonate/2-hydroxyethyl acrylate [HEA]) and pH-responsive P3 gels (HEA/acrylic acid) (Figure 5B–D).[168] Each design exhibits programmable shape changes, such as bending or folding, and can be disassembled with light for reconfiguration.

In the temperature-responsive P2 gel, LCST behavior causes swelling at low temperatures (25°C) due to the zwitterionic moiety, whereas heating (70°C) drives dehydration via enhanced hydrophobic interactions, resulting in shrinkage and deswelling. Within the pH-responsive P3 gel, activation occurs through ionization of carboxylic acid groups from acrylic acid. At high pH (e.g., pH 10), swelling occurs due to deprotonation, generating negatively charged carboxylate ions that increase electrostatic repulsion and osmotic pressure (Figure 5C). At low pH (e.g., pH 4), protonation neutralizes the groups, reducing repulsion and inducing shrinkage.[168] Due to significant variations in swelling ratios, stable pH-triggered motions are sustained over multiple cycles. While no cytotoxicity or viability assessments were explicitly stated, photoactive Ru(II) polypyridyl complexes, often used in photodynamic therapy for cancer, can be cytotoxic in non-targeted contexts; however, polymer encapsulation reduces leaching.[215–217] Although direct analyses of P1, P2, and P3 gel toxicity or cell viability were not performed, composite derivatives similar to these formulations have shown low cytotoxicity and cell viability exceeding 80%.[218–221]

3.1.6. Ionic-responsive materials for extracellular matrix-mimetic remodeling

Ionic-responsive materials—such as polyelectrolyte hydrogels (CS, alginate, or HA with tunable ionizable groups) and ionogels (polymer matrices infused with ionic liquids)—undergo physical or chemical changes, including swelling, contraction, gelation, or phase transitions, in response to ionic stimuli such as salt concentration, specific ions (e.g., Fe^{3+}, citrate), or environmental ionic strength.[222,223] These materials emulate the charge-screening and Donnan osmotic behaviors of native ECM GAGs (e.g., aggrecan and hyaluronan in cartilage or intervertebral disc), where physiological shifts in Na^+, Ca^{2+}, or K^+ concentration rapidly induce reversible swelling/deswelling and stiffness modulation, enabling printed constructs to mimic load-dependent hydration, fixed-charge density changes during skeletal growth, and ionic homeostasis-driven tissue remodeling in electrically active environments such as cardiac or neural niches.[224]

Ionic activation relies on ion–polymer interactions that alter network structure, solubility, or crosslinking, through Donnan equilibrium/osmotic swelling, Hofmeister effect (salting in/out), metal–ion coordination/redox switching, and electrochemical/iontronic effects.[223,225–227] In polyelectrolyte gels like ionized PNIPAAm, fixed charges create ion imbalances, facilitating osmotic swelling in low-ionic-strength solutions, whereas at high ionic strength, charge screening reduces repulsion, causing deswelling.[223,228] Ionic-responsive materials generally exhibit high cell viability and low toxicity due to their natural origin; however, as with any other SMART material, viability and toxicity can be affected by crosslinking concentrations when cells are present.[176,222,223]

In poly(vinyl alcohol) (PVA)/CNF hydrogels, kosmotropic ions ($citrate^{3-}$) polarize water, promoting polymer dehydration and crystallization. Citrate induces gradient densification via hydrogen-bond enhancement, while chaotropic ions (Cl^-) hydrate chains to maintain solubility (Figure 6A–C).[229–231] These properties have been used to create self-healing ionogels that are tunable by ion type and concentration for controlled stiffness gradients.[223,232,233]

This hierarchically heterogeneous PVA/CNF hydrogel—composed of PVA and CNFs—is fabricated via a sequential self-assembly process using directional freezing to align polymer chains and CNFs into honeycomb-like structures, followed by prestretch-assisted salting out in sodium citrate solution.[232] This yields a heterogeneous core–sheath architecture with a compact, highly crosslinked sheath (~23.2 wt% swollen) encasing an aligned porous core featuring belt-like bundles that mimic hierarchical micro- and nanofibrils (Figure 6D and E).[232] This hydrogel surpasses most hydrogels, elastomers, and natural materials by exhibiting exceptional mechanical properties, including tensile strength (55.3 MPa), stiffness (9.5 MPa), stretchability (3300%), toughness (1031 $MJ{\cdot}m^{-3}$), fracture energy (552.7 $kJ{\cdot}m^{-2}$), and fatigue threshold (40.9 $kJ{\cdot}m^{-2}$) (Figure 6F).[232]

The hydrogel also supports regeneration via swelling–resalting, enhances toughness to 1898 $MJ{\cdot}m^{-3}$ over 10 cycles, and exhibits rapid adhesion, making it suitable for cartilage, tendons, or artificial muscle applications (Figure 6G and H). Although no cell viability assessment was performed, the toxicity profile of this hydrogel can be inferred as very low, given that PVA is inherently non-toxic and that CNF (from cellulose) is also biocompatible.[223,230,231]

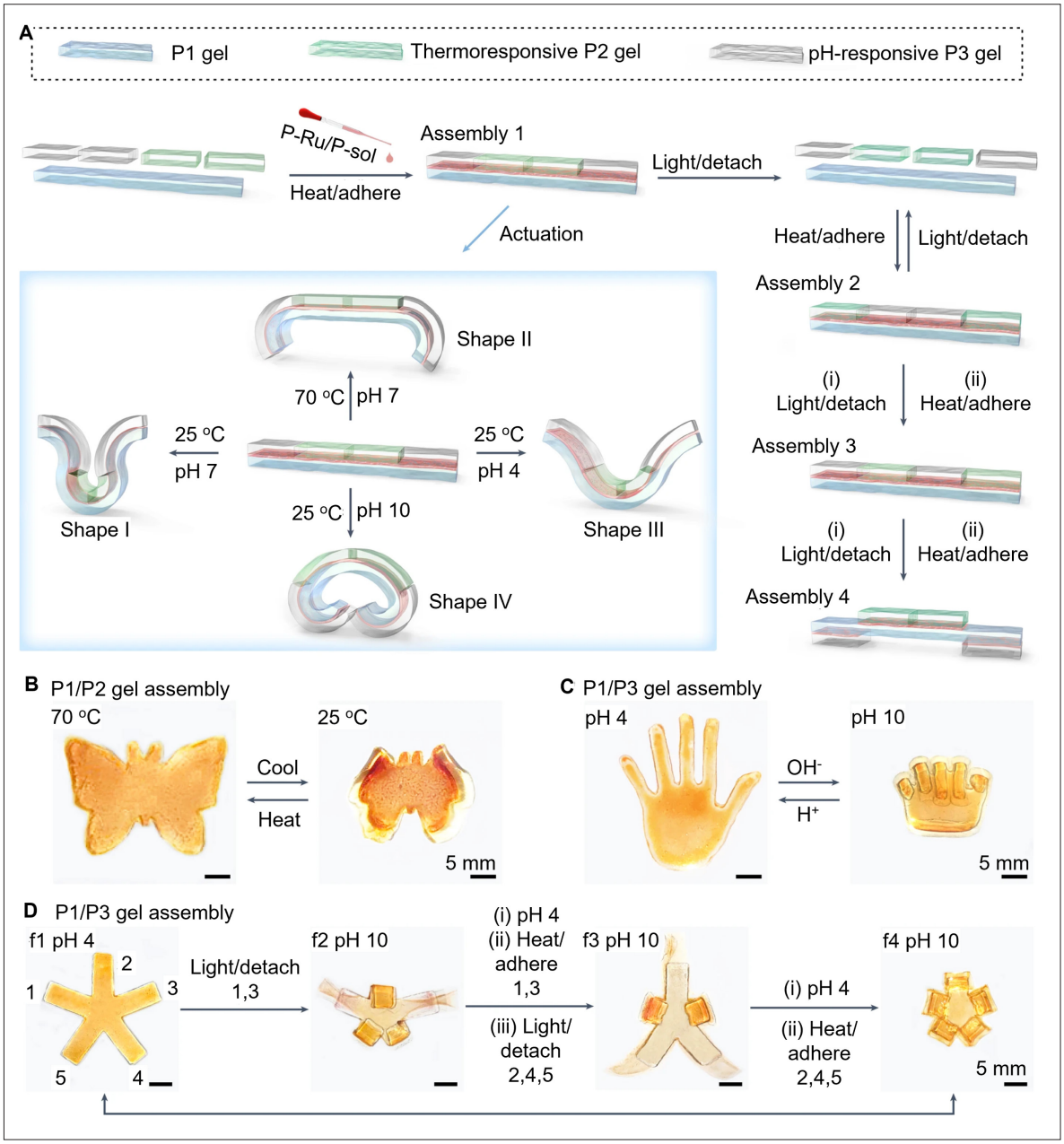

Figure 5. Multi-responsive stimuli-responsive materials for advanced regenerative technologies (pH, light, and temperature). (A) Schematic of hydrogel constructs with complex architectures, illustrating their morphing behavior under varying thermal and pH conditions. Five hydrogel components are linked via the P-Ru/P-S binder to form Construct 1, which can be reorganized into Constructs 2–4. Each construct is capable of transforming into four distinct configurations depending on its design. (B) Actuation of a butterfly-like P1/P2 hydrogel construct in response to different temperatures. (C) Images showing pH-induced actuation of a hand-like P1/P3 hydrogel construct. (D) Selective reversible uncoupling and recoupling of limbs in a five-limbed P1/P3 hydrogel construct, with corresponding actuation under varying pH conditions. Adapted from Ref. [168]

3.1.7. Magnetic-responsive materials for dynamic microenvironment

Magnetic-responsive materials incorporating magnetic nanoparticles (MNPs) such as iron oxide (Fe_3O_4) undergo magnetostriction (shape change) and torque alignment (particles aligning along field lines) through the movement of magnetic domains within the material when subjected to an external magnetic field.[179,234] These materials reproduce the rapid mechanical perturbations transmitted through the ECM during muscle contraction or hemodynamic shear, facilitating cyclic loading that mimics physiological compressive and tensile cues guiding

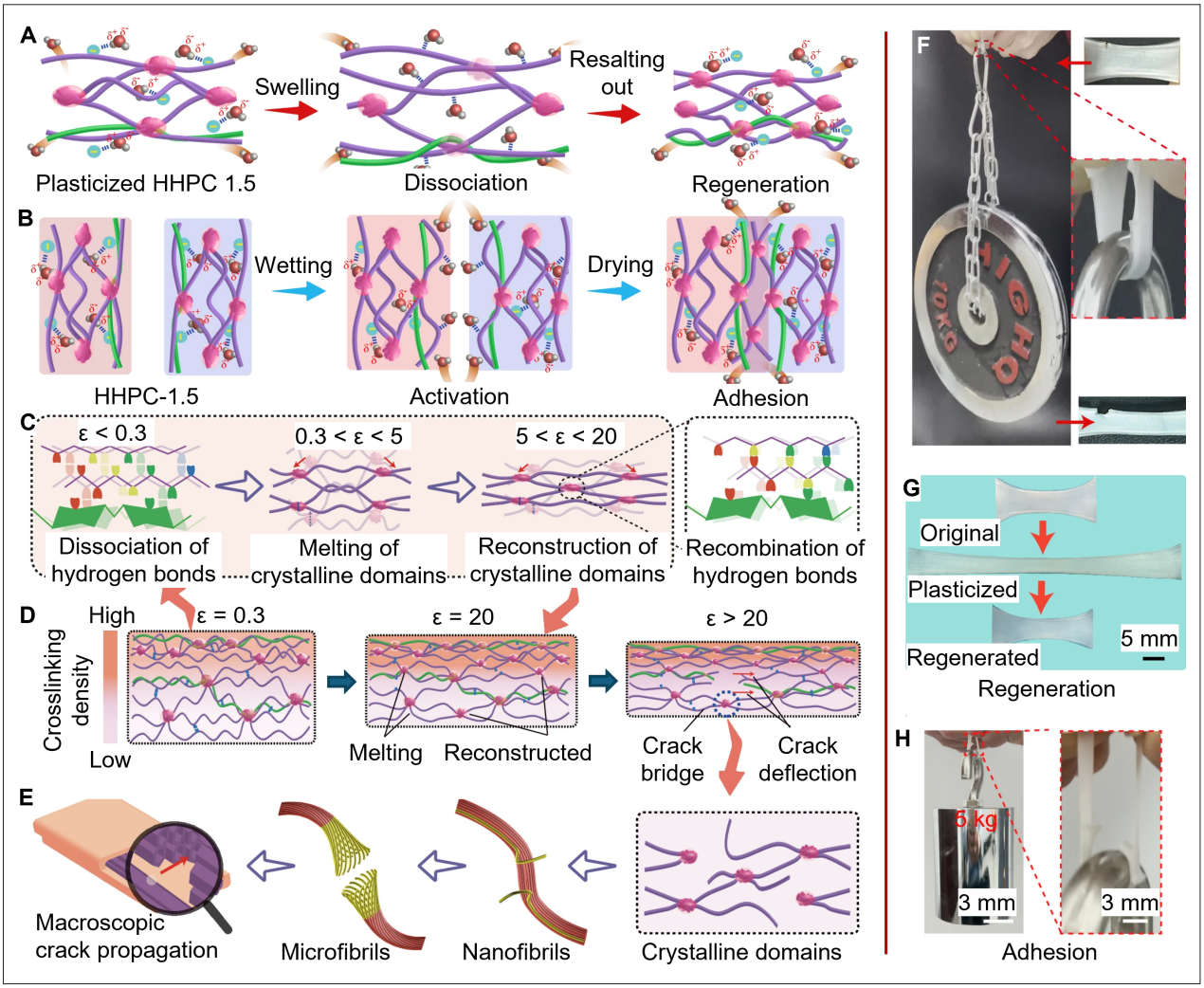

Figure 6. Ionic self-healing hierarchically heterogenous poly(vinyl alcohol)/cellulose nanofibrils (HHPC) hydrogel for regenerative applications. (A) Schematic illustration of the hydrogel regeneration process via breakdown and reconstruction of crystalline structures, driven by interactions between water molecules and kosmotropic ions. (B) Polymer strand mobilization on the densely packed exterior facilitates bonding through hydrogen-bond interactions between water and polymer chains. (C) Synergistic toughening via sheath-led energy absorption, achieved through dissolution and reformation of crystalline regions. (D) Core-led crack-tip passivation through bridging and redirection of fractures. (E) Multi-level energy dissipation via sequential disruption of crystalline regions, nanofibrils, and microfibrils prior to large-scale fracture. (F) HHPC-1.5 hydrogel (~0.4 mm thick) with a 20% pre-cut notch supporting a 10 kg load without crack propagation. (G) Restoration of a deformed HHPC-1.5 hydrogel from a 2 mm clamp spacing via the regeneration procedure. (H) Three HHPC-1.5 hydrogel segments bonded over a 50 mm^2 contact area, sustaining a 5 kg load. Reprinted with permission from Ref. [232] Copyright © 2025, Xu *et al.*

osteogenesis and myogenesis.[235,236] Embedded MNPs are generally nontoxic when encapsulated (PEGylation); however, uncoated MNPs can reduce cell viability and induce lysosomal damage.[237] Another class of magnetic-responsive materials, superparamagnetic nanoparticles, enables pulsatile responses through alternating magnetic fields (100–500 kHz), generating heat via Néel or Brownian relaxation to trigger drug release or hyperthermia.[238,239] These materials support dynamic functionality for guided cell assembly and controlled drug delivery, addressing the common limitations of static tissue-engineering scaffolds.

As shown in Figure 7A, Daul *et al.*[179] used magnetic origami scaffolds with embedded Fe_3O_4 MNPs to integrate bioprinting with ferromagnetism, providing a versatile platform for mimicking dynamic 3D microenvironments. This magnetostriction, activated by exposure to an external field, alters scaffold geometry, creating tapered channels and generating subsequent gravitational cues from folding, which facilitate mechanotransduction and heterogeneous

cell interactions between NIH/3T3 fibroblasts and A549 cancer cells (Figure 7B).[179] An intermediate ECM hydrogel layer modulated cell interactions and proliferation, reduced shear, and enhanced nutrient gradients and media flow for cell guidance between scaffold layers. In these origami scaffolds, iron ion leaching—common with embedded Fe_3O_4 MNPs—remained below toxic levels (100 ppm), maintaining cell viability above 94% over seven days.[179,240]

3.1.8. Electroactive materials for dynamic tissue interfaces

Electro-responsive (electroactive) materials convert electrical energy into mechanical work or vice versa, enabling dynamic interactions with biological systems.[241] These materials emulate the electromechanical coupling and charge-propagation properties of native ECM in excitable tissues (e.g., collagen-mediated piezoelectricity in bone, pericardium, and tendons, or GAG/perlecan-mediated ion channeling in myocardium and nerve), enabling printed constructs to undergo rapid stiffness modulation, directional alignment, or shape change in response to physiological-range electric fields (~1–100 mV/mm).[241–244] They are generally classified into types such as conducting polymers, piezoelectric polymers, and electroactive hydrogels/composites.[242,243,245,246] Conducting

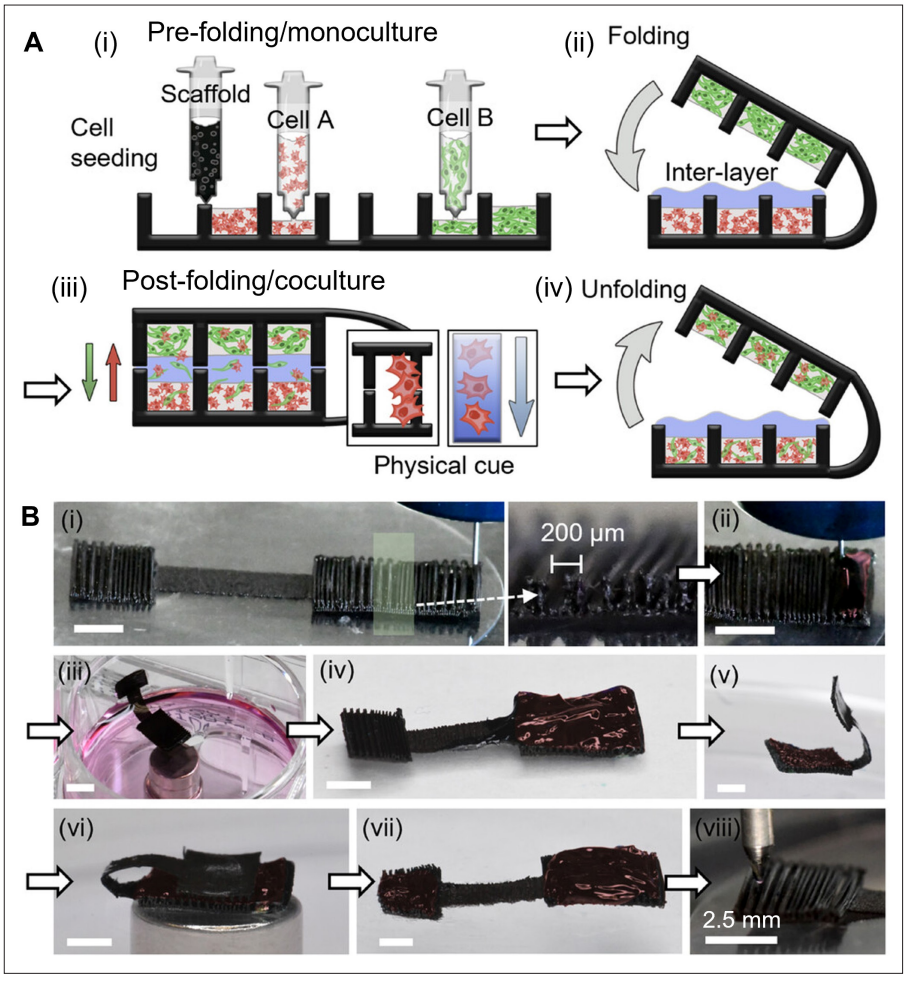

Figure 7. Magnetic-responsive origami platform for guided tissue assembly. (A) Schematic illustration of the experimental workflow for the magnetic-responsive platform: (i) sequential three-dimensional (3D) printing of the scaffold followed by monoculture seeding with cancer cells (red) and fibroblasts (green) prior to folding; (ii) application of hydrogel to form an intermediate extracellular layer between scaffold segments; (iii) formation of a post-folding coculture system, allowing cell clusters to migrate through the intermediate extracellular layer between scaffold sections, guided by scaffold geometry and gravity; and (iv) unfolding of the platform upon magnet removal to assess cell proliferation. (B) Experimental images illustrating each step: (i) 3D printing of the platform with 200 μm channel widths; (ii) cell seeding within microchannels; (iii) pre-folding culture of the seeded scaffold; (iv) application of the intermediate extracellular layer to the bottom scaffold section; (v) magnetic folding of the platform; (vi) post-folding cell culture; (vii) platform unfolding via magnet removal; and (viii) bioindentation analysis of the constructs. Reprinted from Ref. [179]

polymers—including polypyrrole (PPy), PANi, and polythiophene derivatives such as PEDOT:PSS—conduct electricity through conjugated π-electron systems (delocalized electrons due to overlapping p-orbitals) and can be doped to enhance conductivity.[242,247]

Conductive variants (e.g., PEDOT:PSS, MXene, or carbon-nanotube composites) simultaneously mimic the low-resistance extracellular pathways that facilitate synchronous cardiomyocyte contraction, axonal action-potential guidance, and piezo-stimulated osteogenesis observed in load-bearing and neural tissues.[23,25,248] Common conducting polymer composites (e.g., PEDOT:PSS/PPy composites) have enabled stimuli-responsive constructs capable of voltage-triggered swelling or drug release while enhancing mechanical flexibility and biocompatibility.

Piezoelectric polymers, including PVDF and its copolymers (e.g., PVDF-trifluoroethylene, polyhydroxyalkanoates, and poly(L-lactic acid)), generate electric charges under mechanical stress or undergo deformation in response to electric fields, mimicking bioelectricity observed in tissues such as bone and providing piezoelectricity cues for tissue remodeling.[24,242,243] A key advantage of piezoelectric polymers is their ability to transduce mechanical signals into electrical cues, influencing mechanosensitive cellular components, such as ion channels and integrins. This promotes osteogenesis, chondrogenesis, or neural repair without requiring external power sources.[24,181,249] No significant immune responses have been reported in piezoelectric materials, with cell viability maintained above 95% in nerve repair applications.[24]

These materials mimic the hydrated, charged environment of the ECM, which influences biophysical components such as gap junctions for synchronized cell signaling. Electroactive hydrogels and composites integrate responsive elements (conductive fillers like graphene, metallic nanoparticles, or carbon nanotubes) into hydrated networks (e.g., alginate, HA) to enable tunable conductivity and swelling.[243,245] Electroactive materials excel in soft tissue applications due to their material properties, which can be precisely tuned via composite design.[243,245] Similar to MNPs, the toxicity of hydrogels and composites depends on material leaching and the concentration and type of conductive filler used to enable electroactive/electroresponsive properties.[241,242]

Together, these stimulus classes—and their deliberate integration—provide a framework for 4D bioprinting, where material responsiveness is matched to biological timescales and microenvironmental cues, enabling on-demand morphing, signal delivery, and cell-instructive remodeling while maintaining the strict biocompatibility and stability required for translational applications.

3.2. Comparative overview of stimuli-responsive materials

With these foundational insights into native ECM dynamics and the evolving portfolio of ECM-inspired 4D SMART materials, we now present a comparative analysis of the principal stimulus-responsive classes, along with a critical assessment of their readiness and remaining barriers to clinical translation. As noted earlier, conventional 3D bioprinting yields static constructs whose geometry, stiffness, porosity, and bioactivity are fixed upon deposition, with any subsequent evolution limited to passive degradation or non-programmed cell-mediated remodeling.[16] In contrast, 4D bioprinting harnesses stimuli-responsive bioinks engineered for precise, triggerable actuation—manifesting as controlled folding, twisting, swelling/deswelling, stiffening/softening transitions, anisotropic alignment, or spatially resolved porosity changes—in direct response to biophysical and biochemical cues (e.g., temperature, pH, ionic strength, light, electric/magnetic fields, enzymes, or metabolites).[12]

These engineered actuation mechanisms enable 4D SMART systems to emulate previously inaccessible ECM dynamics, including on-demand curvature-driven morphogenesis, cyclic strain-induced fiber alignment, hydration-gated permeability transitions, localized enzyme-triggered remodeling, and cell-force–amplified shape evolution.[250] In doing so, they deliver autonomous, self-organizing tissue behaviors that remain unattainable with static 3D bioprinted scaffolds. Direct comparison of these 4D approaches (Table 3) provides further insight into their current ECM fidelity, clinical translation progress, representative applications where dynamic responsiveness consistently outperforms static 3D bioprinting, and the critical limitations that remain the principal barriers to widespread clinical adoption.

Thermo-responsive hydrogels (predominantly PNIPAAm copolymers) remain the most widely adopted class due to printing compatibility and decades of safety data from non-printed devices. They reliably mimic temperature-driven collagen remodeling and wound-stiffening trajectories (1–100 kPa over days), driving robust chondrogenic and corneal epithelial differentiation in organoids.[251] Nevertheless, their slow response kinetics (>5 min), hysteresis, and persistent concerns over residual NIPAAm monomer cytotoxicity continue to restrict them to preclinical cartilage and ocular trials.[252,253]

Table 3. Cross-comparison of stimuli-responsive SMART materials in 4D bioprinting

Stimulus class	**Closest native ECM behavior mimicked**	**Spatio-temporal control vs. ECM**	**Reversibility and speed vs. ECM**	**Long-term *in vivo* stability**	**Multi-stimuli integration capability**	**Regulatory feasibility**	**Clinical translation stage**	**Near-term *ex vivo* application**	**Ref**
Thermo-responsive	Collagen remodeling, wound maturation	Medium (whole-construct)/poor match	Good/100–1000 times slower than ECM	4–8 weeks (monomer leaching)	Moderate (thermo+pH common)	Moderate (PNIPAAm history in devices)	Preclinical	Stiffness-maturation models (cartilage, cornea)	[5,7,184,185,251–253]
pH-responsive	Inflammation-driven fibrosis	Regional/reasonable match	Poor reversibility	<4 weeks (pH drift, degradation)	High	Low (cell damage risk)	Preclinical only	Tumor microenvironment platforms	[7,189–191,254,255]
Light-responsive	Ultraviolet-dermal remodeling, reactive oxygen species signaling	Highest precision/ excellent local match	High or irreversible	2–6 weeks (photoproduct accumulation)	High (light+thermo widespread)	Low (phototoxicity data scarce)	Preclinical	Vascular branching and perfusion models	[205,207,208,256–261]
Magnetic-responsive	Hemodynamic shear, muscle loading	Whole-construct/ good mechanical match	Excellent/near-ECM speed	6–12 weeks (iron oxidation)	Moderate	Very low (metal particles)	Preclinical	Dynamic soft robotics	[179,235,236,262,263]
Ionic-responsive	Cartilage GAG fixed-charge swelling	Diffusion-limited/ very close chemically	Excellent/Near-ECM	4–8 weeks (ion leaching)	High	Moderate	Early preclinical	Osteoarthritis and disc degeneration models	[222–225,264–266]
Electro-/ conductive	Myocardial conduction, bone piezoelectricity	Directional/closest functional match	Excellent/ECM-like mechanical response	3–12 months (best in class)	High	Highest (ongoing phase I)	Phase I human trials (cardiac patches)	Cardiac patches and *ex vivo* heart-on-chip	[24,241–248,267–269]
Hydration-responsive	Interstitial fluid shifts, corneal swelling	Passive/good osmotic match	Slow but reversible	>12 weeks (inert polymers)	Very high (bilayer combinations)	High (no exogenous energy)	Preclinical (bilayer tubular grafts)	Barrier tissues and simple tubular grafts	[199–203,270–272]
Multi-responsive	Developmental folding, wound progression	Highest complexity/ closest to real ECM	Variable, often reduced	Worst (compounded degradation)	Intrinsic	Lowest (combination product)	Furthest from clinical translation	Complex disease and developmental models	[5,7,9,21,208]

Abbreviations: ECM: extracellular matrix; GAG: glycosaminoglycan; PNIPAAm: poly(*N*-isopropylacrylamide).

pH-responsive polymers effectively model pathological acidification (e.g., tumor stroma, chronic wounds), producing localized stiffening and drug-release zones that drive realistic cancer cell invasion.[254] Nonetheless, their narrow safe triggering window and irreversible drift in physiological buffers severely limit in vivo utility and keep them in preclinical drug-delivery rather than structural 4D applications.[255]

Hydration/water-responsive bilayers represent the simplest and safest route to 4D behavior. By exploiting differential swelling of hydrophilic polymers (e.g., poly(ethylene glycol)) diacrylate versus poly(hydroxyethyl methacrylate)), they passively self-fold into tubes or open porous networks upon immersion in aqueous media, closely imitating diurnal hydration shifts in skin and cornea.[270,271] Applications directed toward urethral and small-vessel models can roll into perfusable conduits within hours without exogenous energy, offering a clear advantage over manual suturing or sacrificial templating required in 3D bioprinting.[272] However, actuation remains slow (hours–days) and difficult to program precisely, but the absence of toxic triggers provides this class with one of the highest regulatory feasibility scores.

Light-responsive systems provide unparalleled spatiotemporal precision (sub-100 μm) through photo-isomerization (e.g., azobenzene) or photocleavage (e.g., o-nitrobenzyl) mechanisms,[256] enabling on-demand vascular branching and topographical reconfiguration that mimics angiogenic sprouting and dermal remodeling.[257,258] A striking *ex vivo* demonstration used visible-light-triggered spiropyran-containing hydrogels to create self-bending cardiac microtissues.[259,260] Upon blue-light patterning, localized softening induced anisotropic curvature, directing cardiomyocyte alignment and producing spontaneously beating helical bundles within five days. This outcome remains unattainable in rigid 3D GelMA constructs, which yield only isotropic monolayers.[261] Despite this precision, limited penetration depth (less than 1 mm for visible light, approximately 1 cm for NIR), phototoxicity from prolonged exposure, and NIR-induced hyperthermia continue to confine clinical applications to thin tissues or *ex vivo* platforms.[205,256]

Ionic-responsive systems exhibit the closest chemical mimicry of GAG-rich matrices such as articular cartilage and intervertebral disc. Alginate- and hyaluronan-based inks crosslinked by physiological Ca^{2+} or Mg^{2+} concentrations reproduce the fixed-charge density and Donnan osmotic pressure with near-native accuracy, producing reversible 50–300% volume changes under load.[264] *Ex vivo* intervertebral disc models subjected to diurnal ionic cycles maintain height and modulus for over eight weeks, whereas static 3D alginate collapses within days.[265,266]

Magnetic-responsive ferrogels excel at delivering remote, penetration-unlimited mechanical stimulation with sub-second response times, effectively replicating physiological cyclic compression in bone and cartilage or hemodynamic shear in vascular niches.[262] A representative *ex vivo* application employed magnetic-field-guided crawling constructs seeded with mesenchymal stem cells to create self-navigating soft robots that actively compact and remodel printed collagen matrices, achieving 5.3 times higher alkaline phosphatase activity and mineralized nodule formation within 14 days compared with identical but non-actuated 3D controls.[263,273] Despite these capabilities, long-term oxidative release of iron ions, particle aggregation, chronic inflammation, and magnetic resonance imaging incompatibilities remain insurmountable barriers to clinical translation.

Electro-conductive materials currently deliver the highest functional ECM fidelity for excitable tissues. By restoring low-resistance pathways (10^{-3}–10^{1} S/cm) and true electromechanical coupling, they enable synchronous cardiomyocyte contraction, action-potential propagation in neuronal networks, and piezoelectric-like signaling in bone—capabilities entirely absent in insulating 3D-printed scaffolds.[267,268] This has translated directly into the most advanced clinical status, with multiple phase I human trials for conductive cardiac patches ongoing, and 3-to-12-month electrode stability already demonstrated in large-animal models.[269] The dominant remaining limitations are delamination at the bioelectronic interface and chronic inflammation triggered by conductive polymer degradation. These remain significant but are actively being addressed with biodegradable alternatives (e.g., PEDOT–lignin).[268]

This proposed hierarchy provides a realistic translational roadmap for 4D bioprinting. Looking forward, the years 2026–2030 will likely yield the first regulatory-approved 4D products, namely electro-conductive cardiac and nerve patches, together with hydration- and thermo-responsive self-assembling tubular grafts. From 2030 to 2035, hybrid ionic–electronic constructs suitable for joints and myocardium are expected to reach clinical application. Multi-responsive, fully vascularized tissues capable of true organ replacement are the furthest from realization and will likely not emerge until after 2035, once robust, orthogonal, and degradation-resistant chemistries become available. Until then, the primary clinical value of 4D bioprinting will lie in its capacity to generate dynamic, human-relevant models and minimally complex dynamic implants rather than in whole-organ reconstruction.

4. Conclusion, technical challenges, and outlook

Looking forward, the unification of each respective domain (physics, biology, chemistry, engineering, and medicine) has become central to the evolution of future research in 4D bioprinting and 4D tissue engineering. These emerging outcomes facilitate 4D SMART materials to advance from proof-of-concept demonstrations toward tangible applications across the translational spectrum. *In vitro*, multi-responsive (pH, thermo, and light) tumor models that sequentially stiffen and fold over 7–14 days predict metastasis 2–3 times more accurately than static 3D cultures.[3,214,219,274] *Ex vivo*, bone and cartilage scaffolds change shape or stiffness in response to physiological conditions, while electro-conductive cardiac patches enable high-fidelity arrhythmogenic studies.[8,91,138]

Clinically, electro-conductive cardiac patches (PEDOT:PSS/GelMA) are in phase I human trials for post-infarction conduction restoration, while large-animal preclinical studies show 8–12-week survival of thermo-responsive, self-folding tracheal tubes, and hydration-driven self-rolling vascular grafts.[8,145,169,268,275] Although no 4D-printed solid organ has reached human transplantation, the technology already delivers its greatest near-term impact through advanced human disease models for precision medicine and through restoration of dynamic electrical and mechanical function in thin, excitable tissues.

Using this shift in perspective, radical breakthroughs, such as the development of bioreactors for functional, human-scale tissues and organ transplantation, could potentially be realized.[13,276] These advances will realign scientific incentives for bolder experimentation to address the stagnation of specialization approaches.[255,277] However, radical developments can only come after we address current challenges and limitations in each respective domain. 4D bioprinting and tissue engineering processes are inherently more complex than 3D methods due to the requirements for precise spatiotemporal control over dynamic transformations of the SMART materials used. Having previously covered SMART material mechanical properties that fail to fully mimic the multi-responsive *in vivo* environment and their poor cytocompatibility, we will conclude this review by addressing the constraints of the printing process and how printability, scaling, and regulatory considerations have brought the field to its current state.[2,140,277,278]

From a technological standpoint, one of the most persistent challenges lies in print resolution and fidelity. Existing extrusion-based bioprinters typically achieve feature sizes of 100–200 μm, which remain too coarse to reproduce the intricate microvascular networks required for nutrient diffusion in tissues such as skin, myocardium, or vasculature.[279] This limitation often results in hypoxic cores and reduced construct viability beyond 1–2 mm thickness.[250] While extrusion-based methods continue to dominate, they also struggle to achieve high throughput and scalability for human-scale tissues.

In contrast, laser-guided or coaxial printing offers precision but at higher costs and even lower throughput.[280] In 4D contexts, maintaining fidelity during dynamic changes is difficult, as materials may warp unpredictably post-print. This limits the formation of heterogeneous skin structures with adaptive porosity and cardiac patches that mimic curvature.[145,281] Emerging multi-nozzle systems and 6D robotic bioprinting systems significantly mitigate these limitations by incorporating multi-material deposition, three rotational axes (pitch, yaw, roll) alongside translational ones, and enabling unprecedented flexibility in orientation and path planning.[282,283] Automation of these systems aims to synchronize extrusion with robotic motion, potentially boosting speed and reproducibility while maintaining cell viability and functionality, thereby advancing toward clinical translation.[250,283]

However, technological progress alone is insufficient without a parallel evolution in regulatory and ethical frameworks. At present, regulatory systems for 4D bioprinting remain underdeveloped, relying heavily on precedents set for 3D bioprinting and traditional medical devices. This mismatch leads to ambiguous product classifications, delayed approvals, and uncertainties in clinical translation.[284–286] In the United States, the Food and Drug Administration classifies bioprinted constructs as combination products—integrating biologics, devices, and drugs—subjecting them to rigorous premarket approval under 21 CFR Parts 1270–1271 for human cells, tissues, and products (HCT/Ps).[287,288] However, it currently lacks specific guidelines for 4D dynamic materials, leaving uncertainty around long-term safety and performance in applications.[289]

In the European Union, the Medical Device Regulation 2017/745 governs custom-made devices under Article 2(3) and Annex XIII 277, which categorize high-risk bioprinted implants as Class III, but struggle to address customized 4D products, raising legal challenges, including risk assessment and conformity.[290] The European Medicines Agency regulates 4D bioprinted tissues under Regulation EC No 1394/2007 on advanced therapy medicinal products,[291] requiring rigorous clinical trials and safety or efficacy data.[292] However, it overlooks SRMs, and globally, these gaps contribute to slow commercialization, resulting

in only one bioprinted ear in trials as of 2025.[293] The World Health Organization has called for harmonized standards; however, disparities persist,[294] with stricter European Union regulations contrasting with more flexible approaches in the United States.[284,286] This lack of international consensus on standards for stimuli-responsive devices poses a risk of unintended *in vivo* transformations, potentially violating safety protocols under national laws such as the United Kingdom's Human Tissue Act (2004).[8,290,295]

Given these substantial obstacles, the translation of 4D bioprinting from bench to bedside continues to lag by 5–10 years behind laboratory advances. Technical limitations constrain scalability and reproducibility, while regulatory uncertainty prolongs validation and licensing, forming a bottleneck that stifles clinical innovation.[8,255] To overcome these challenges, the field requires coordinated global reform—including updated Food and Drug Administration/European Medicines Agency joint guidelines tailored to 4D systems, interdisciplinary regulatory boards that integrate material scientists and clinicians, and international standardization efforts led by the World Health Organization and the International Organization for Standardization.[284,292,294] Only through such harmonization can researchers and policymakers ensure the safe and accelerated translation of adaptive, living biomaterials into the clinic. By aligning technological readiness with ethical and legal accountability, 4D bioprinting may finally progress from conceptual promise to a practical platform for regenerative medicine and human-scale tissue replacement.

Acknowledgments

None.

Funding

This research was supported by the Commonwealth Health Research Board (236-08-21); the National Institutes of Health, under the National Institute of General Medical Sciences grant (P20GM113126); the American Cancer Society (IRG-22-146-07-IRG); National Institutes of Health, under the National Cancer Institute grant (CA036727), the Nexus of Virology, Immunology, and Bioengineering; the Nebraska Tobacco Settlement Biomedical Research Development Funds; the "Regional Innovation System & Education (RISE)" program, through the Gwangju RISE Center, funded by the Ministry of Education and the Gwangju Metropolitan Government, Republic of Korea (2025-RISE-05-011).

Conflict of interest

Fanben Meng and Daeha Joung serve as the guest editors of this Special Issue, but did not in any way involve in the editorial and peer-review process conducted for this paper, directly or indirectly. Other authors declare they have no competing interests.

Author contributions

Conceptualization: Ryan Martin, Daeha Joung
Writing–original draft: Ryan Martin, Haiwei Zhai, Fanben Meng, Daehoon Han,
Writing–review & editing: Ryan Martin, Fanben Meng, Daeha Joung

Ethics approval and consent to participate

Not applicable.

Consent for publication

Not applicable.

Availability of data

Not applicable.

References

1. Crossley RM, Johnson S, Tsingos E, *et al*. Modeling the extracellular matrix in cell migration and morphogenesis: a guide for the curious biologist. *Front Cell Dev Biol*. 2024;12:1354132.
doi: 10.3389/fcell.2024.1354132

2. Martin R, Joung D. The promise and challenges of bioprinting in tissue engineering. *Micromachines*. 2024;15(12):1529.
doi: 10.3390/mi15121529

3. Lu P, Ruan D, Huang M, *et al*. Harnessing the potential of hydrogels for advanced therapeutic applications: current achievements and future directions. *Signal Transduct Target Ther*. 2024;9(1):166.
doi: 10.1038/s41392-024-01852-x

4. Dethe MR, Prabakaran A, Ahmed H, Agrawal M, Roy U, Alexander A. PCL-PEG copolymer based injectable thermosensitive hydrogels. *J Control Release*. 2022;343:217-236.
doi: 10.1016/j.jconrel.2022.01.035

5. Doberenz F, Zeng K, Willems C, Zhang K, Groth T. Thermoresponsive polymers and their biomedical application in tissue engineering – a review. *J Mater Chem B*. 2020;8(4):607-628.
doi: 10.1039/C9TB02052G

6. Pei Y, Chen J, Yang L, *et al*. The effect of pH on the LCST of poly(N-isopropylacrylamide) and poly(N-isopropylacrylamide-co-acrylic acid). *J Biomat Sci Polymer Edn*. 2004;15(5):585-594. doi: 10.1163/156856204323046852

7. Correa S, Grosskopf AK, Lopez Hernandez H, *et al*. Translational applications of hydrogels. *Chem Rev*. 2021;121(18):11385-11457. doi: 10.1021/acs.chemrev.0c01177

8. Taylor S, Mueller E, Jones LR, Makela AV, Ashammakhi N. Translational aspects of 3D and 4D printing and bioprinting. *Adv Healthc Mater.* 2024;13(27):2400463. doi: 10.1002/adhm.202400463

9. Cao H, Duan L, Zhang Y, Cao J, Zhang K. Current hydrogel advances in physicochemical and biological response-driven biomedical application diversity. *Signal Transduct Target Ther*. 2021;6(1):426. doi: 10.1038/s41392-021-00830-x

10. Di X, Gao X, Peng L, *et al*. Cellular mechanotransduction in health and diseases: from molecular mechanism to therapeutic targets. *Signal Transduct Target Ther*. 2023;8(1):282. doi: 10.1038/s41392-023-01501-9

11. Ambattu LA, Yeo LY. Sonomechanobiology: vibrational stimulation of cells and its therapeutic implications. *Biophys Rev.* 2023;4(2):021301. doi: 10.1063/5.0127122

12. Arif ZU, Khalid MY, Ahmed W, Arshad H. A review on four-dimensional (4D) bioprinting in pursuit of advanced tissue engineering applications. *Bioprinting*. 2022;27:e00203. doi: 10.1016/j.bprint.2022.e00203

13. Zhou W, Chen Y, Roh T, *et al*. Multifunctional bioreactor system for human intestine tissues. *ACS Biomater Sci Eng*. 2018;4(1):231-239. doi: 10.1021/acsbiomaterials.7b00794

14. Williamson A, Khoshmanesh K, Pirogova E, *et al*. Bioreactors: a regenerative approach to skeletal muscle engineering for repair and replacement. *Adv Nanobiomed Res*. 2024;4(10):2400030. doi: 10.1002/anbr.202400030

15. Yarali E, Mirzaali MJ, Ghalayaniesfahani A, Accardo A, Diaz-Payno PJ, Zadpoor AA. 4D printing for biomedical applications. *Adv Mater.* 2024;36(31):2402301. doi: 10.1002/adma.202402301

16. Wang J, Wang Y, Wang R, *et al*. A review on 3D printing processes in pharmaceutical engineering and tissue engineering: applications, trends and challenges. *Adv Mater Technol.* 2025;10(2):2400620. doi: 10.1002/admt.202400620

17. Joung D, Lavoie NS, Guo S, Park SH, Parr AM, McAlpine MC. 3D printed neural regeneration devices. *Adv Funct Mater.* 2020;30(1):1906237. doi: 10.1002/adfm.201906237

18. Li YC, Zhang YS, Akpek A, Shin SR, Khademhosseini A. 4D bioprinting: the next-generation technology for biofabrication enabled by stimuli-responsive materials. *Biofabrication*. 2016;9(1):012001. doi: 10.1088/1758-5090/9/1/012001

19. Michael PL, Lam YT, Mitchell TC, *et al*. Harnessing physiological shear stress in a perfusion bioreactor for enhanced endothelialization of small-diameter vascular grafts. *Adv Nanobiomed Res*. 2025;5:2500025. doi: 10.1002/anbr.202500025

20. Mierke CT. Viscoelasticity, like forces, plays a role in mechanotransduction. *Front Cell Dev Biol*. 2022;10:789841. doi: 10.3389/fcell.2022.789841

21. Asadi Tokmedash M, Kim C, Chavda AP, Li A, Robins J, Min J. Engineering multifunctional surface topography to regulate multiple biological responses. *Biomaterials*. 2025;319:123136. doi: 10.1016/j.biomaterials.2025.123136

22. Özkale B, Sakar MS, Mooney DJ. Active biomaterials for mechanobiology. *Biomaterials*. 2021;267:120497. doi: 10.1016/j.biomaterials.2020.120497

23. Kayser LV, Lipomi DJ. Stretchable conductive polymers and composites based on PEDOT and PEDOT:PSS. *Adv Mater.* 2019;31(10):1806133. doi: 10.1002/adma.201806133

24. Bryan AE, Krutko M, Rebholz S, *et al*. Development of a bioactive, piezoelectric PVDF-TrFE scaffold with evaluation of tissue reaction for potential in nerve repair. *Biomater Sci*. 2025;13(20):5769-5785. doi: 10.1039/D5BM01054C

25. Mariano A, Lubrano C, Bruno U, Ausilio C, Dinger NB, Santoro F. Advances in cell-conductive polymer biointerfaces and role of the plasma membrane. *Chem Rev*. 2022;122(4):4552-4580. doi: 10.1021/acs.chemrev.1c00363

26. Tonti OR, Larson H, Lipp SN, *et al*. Tissue-specific parameters for the design of ECM-mimetic biomaterials. *Acta Biomater.* 2021;132:83-102. doi: 10.1016/j.actbio.2021.04.017

27. Valdoz JC, Johnson BC, Jacobs DJ, *et al*. The ECM: to scaffold, or not to scaffold, that is the question. *Int J Mol Sci*. 2021;22(23):12690. doi: 10.3390/ijms222312690

28. Rahmati M, Silva EA, Reseland JE, A. Heyward C, Haugen HJ. Biological responses to physicochemical properties of biomaterial surface. *Chem Soc Rev*. 2020;49(15):5178-5224. doi: 10.1039/D0CS00103A

29. Yamada KM, Doyle AD, Lu J. Cell–3D matrix interactions: recent advances and opportunities. *Trends Cell Biol.* 2022;32(10):883-895.

doi: 10.1016/j.tcb.2022.03.002

30. Hervé S, Miroshnikova YA. Biophysical determinants of nuclear shape and mechanics and their implications for genome integrity. *Curr Opin Biomed Eng*. 2024;30:100521. doi: 10.1016/j.cobme.2024.100521

31. Miroshnikova YA, Wickström SA. Mechanical forces in nuclear organization. *Cold Spring Harb Perspect Biol*. 2022;14(1):a039685. doi: 10.1101/cshperspect.a039685

32. Vermeulen S, Honig F, Vasilevich A, *et al*. Expanding biomaterial surface topographical design space through natural surface reproduction. *Adv Mater*. 2021;33(31):2102084. doi: 10.1002/adma.202102084

33. Comelles J, Fernández-Majada V, Acevedo V, Rebollo-Calderon B, Martínez E. Soft topographical patterns trigger a stiffness-dependent cellular response to contact guidance. *Mater Today Bio*. 2023;19:100593. doi: 10.1016/j.mtbio.2023.100593

34. Min K, Karuppannan SK, Tae G. The impact of matrix stiffness on hepatic cell function, liver fibrosis, and hepatocellular carcinoma-based on quantitative data. *Biophys Rev*. 2024;5(2):021306. doi: 10.1063/5.0197875

35. Elosegui-Artola A, Gupta A, Najibi AJ, *et al*. Matrix viscoelasticity controls spatiotemporal tissue organization. *Nat Mater*. 2023;22(1):117-127. doi: 10.1038/s41563-022-01400-4

36. Wu Y, Song Y, Soto J, *et al*. Viscoelastic extracellular matrix enhances epigenetic remodeling and cellular plasticity. *Nat Commun*. 2025;16(1):4054. doi: 10.1038/s41467-025-59190-7

37. Wan S, Chen Y, Huang C, *et al*. Scalable ultrastrong MXene films with superior osteogenesis. *Nature*. 2024;634(8036):1103-1110. doi: 10.1038/s41586-024-08067-8

38. Cheng Y, Wang Y, Wang Y, *et al*. Microenvironment-feedback regulated hydrogels as living wound healing materials. *Nat Commun*. 2025;16(1):6050. doi: 10.1038/s41467-025-60858-3

39. Zhang C, Cai D, Liao P, *et al*. 4D printing of shape-memory polymeric scaffolds for adaptive biomedical implantation. *Acta Biomater*. 2021;122:101-110. doi: 10.1016/j.actbio.2020.12.042

40. Benwood C, Chrenek J, Kirsch RL, *et al*. Natural biomaterials and their use as bioinks for printing tissues. *Bioengineering*. 2021;8(2):27. doi: 10.3390/bioengineering8020027

41. Chen XB, Fazel Anvari-Yazdi A, Duan X, *et al*. Biomaterials/bioinks and extrusion bioprinting. *Bioact Mater*. 2023;28:511-536. doi: 10.1016/j.bioactmat.2023.06.006

42. Carvalho EM, Kumar S. Lose the stress: viscoelastic materials for cell engineering. *Acta Biomater*. 2023;163:146-157. doi: 10.1016/j.actbio.2022.03.058

43. Fonseca AC, Melchels FP, Ferreira MJ, *et al*. Emulating human tissues and organs: a bioprinting perspective toward personalized medicine. *Chem Rev*. 2020;120(19):11093-11139. doi: 10.1021/acs.chemrev.0c00342

44. Khalid MY, Otabil A, Mamoun OS, Askar K, Bodaghi M. Transformative 4D printed SMPs into soft electronics and adaptive structures: innovations and practical insights. *Adv Mater Technol*. 2025;10(19):e00309. doi: 10.1002/admt.202500309

45. Mirasadi K, Yousefi MA, Jin L, *et al*. 4D printing of magnetically responsive shape memory polymers: toward sustainable solutions in soft robotics, wearables, and biomedical devices. *Adv Sci*. 2025:e13091. doi: 10.1002/advs.202513091

46. Zhang W, Liu Y, Zhang H. Extracellular matrix: an important regulator of cell functions and skeletal muscle development. *Cell Biosci*. 2021;11(1):65. doi: 10.1186/s13578-021-00579-4

47. Hynes RO. The extracellular matrix: not just pretty fibrils. *Science*. 2009;326(5957):1216-1219. doi: 10.1126/science.1176009

48. Zhang S-y, Li X-y, Yang N, *et al*. Electrospun collagen nanofibers reduce inflammation, inhibit fibrosis, and promote wound healing on the ocular surface. *ACS Appl Nano Mater*. 2024;7(17):20267-20278. doi: 10.1021/acsanm.4c03180

49. Orr SB, Chainani A, Hippensteel KJ, *et al*. Aligned multilayered electrospun scaffolds for rotator cuff tendon tissue engineering. *Acta Biomater*. 2015;24:117-126. doi: 10.1016/j.actbio.2015.06.010

50. Kim HN, Jiao A, Hwang NS, *et al*. Nanotopography-guided tissue engineering and regenerative medicine. *Adv Drug Deliv Rev*. 2013;65(4):536-558. doi: 10.1016/j.addr.2012.07.014

51. Putra VDL, Kilian KA, Knothe Tate ML. Biomechanical, biophysical and biochemical modulators of cytoskeletal remodelling and emergent stem cell lineage commitment. *Commun Biol*. 2023;6(1):75. doi: 10.1038/s42003-022-04320-w

52. Pike DB, Cai S, Pomraning KR, *et al*. Heparin-regulated release of growth factors in vitro and angiogenic response in vivo to implanted hyaluronan hydrogels containing VEGF and bFGF. *Biomaterials*. 2006;27(30):5242-5251. doi: 10.1016/j.biomaterials.2006.05.018

53. Zhao T, Huang Y, Zhu J, *et al*. Extracellular matrix signaling cues: biological functions, diseases, and therapeutic targets. *MedComm*. 2025;6(8):e70281. doi: 10.1002/mco2.70281

54. Karamanos NK, Theocharis AD, Piperigkou Z, *et al*. A guide to the composition and functions of the extracellular matrix. *FEBS J*. 2021;288(24):6850-6912. doi: 10.1111/febs.15776

55. Nicolas J, Magli S, Rabbachin L, Sampaolesi S, Nicotra F, Russo L. 3D extracellular matrix mimics: fundamental concepts and role of materials chemistry to influence stem cell fate. *Biomacromolecules*. 2020;21(6):1968-1994. doi: 10.1021/acs.biomac.0c00045

56. Liu C, Pei M, Li Q, Zhang Y. Decellularized extracellular matrix mediates tissue construction and regeneration. *Front Med*. 2022;16(1):56-82. doi: 10.1007/s11684-021-0900-3

57. Zhang X, Chen X, Hong H, Hu R, Liu J, Liu C. Decellularized extracellular matrix scaffolds: Recent trends and emerging strategies in tissue engineering. *Bioact Mater*. 2022;10:15-31. doi: 10.1016/j.bioactmat.2021.09.014

58. Xie R, Yu X, Cao T, *et al*. Fibrous viscoelastic extracellular matrix assists precise neuronal connectivity. *Adv Funct Mater*. 2023;33(36):2301926. doi: 10.1002/adfm.202301926

59. Karsdal MA, ed. *Biochemistry of Collagens, Laminins and Elastin: Structure, Function and Biomarkers*. 3rd ed. London. United Kingdom: Academic Press. An imprint of Elsevier; 2024.

60. Wang Z, Liu H, Luo W, *et al*. Regeneration of skeletal system with genipin crosslinked biomaterials. *J Tissue Eng*. 2020;11:2041731420974861. doi: 10.1177/2041731420974861

61. Despanie J, Dhandhukia JP, Hamm-Alvarez SF, MacKay JA. Elastin-like polypeptides: Therapeutic applications for an emerging class of nanomedicines. *J Control Release* 2016;240:93-108. doi: 10.1016/j.jconrel.2015.11.010

62. Wang K, Meng X, Guo Z. Elastin structure, synthesis, regulatory mechanism and relationship with cardiovascular Diseases. *Front Cell Dev Biol*. 2021;9:596702. doi: 10.3389/fcell.2021.596702

63. Dai X, Wu D, Xu K, Ming P, Cao S, Yu L. Viscoelastic mechanics: from pathology and cell fate to tissue regeneration biomaterial development. *ACS Appl Mater Interfaces*. 2025;17(6):8751-8770. doi: 10.1021/acsami.4c18174

64. Tillman BW, Yazdani SK, Lee SJ, Geary RL, Atala A, Yoo JJ. The in vivo stability of electrospun polycaprolactone-collagen scaffolds in vascular reconstruction. *Biomaterials*. 2009;30(4):583-588. doi: 10.1016/j.biomaterials.2008.10.006

65. Shao Y, Fu J. Integrated micro/nanoengineered functional biomaterials for cell mechanics and mechanobiology: a materials perspective. *Adv Mater*. 2014;26(10):1494-1533. doi: 10.1002/adma.201304431

66. Cavalcanti-Adam EA, Aydin D, Hirschfeld-Warneken VC, Spatz JP. Cell adhesion and response to synthetic nanopatterned environments by steering receptor clustering and spatial location. *HFSP J*. 2008;2(5):276-285. doi: 10.2976/1.2976662

67. Longstreth JH, Wang K. The role of fibronectin in mediating cell migration. *Am J Physiol Cell Physiol*. 2024;326(4):C1212-C1225. doi: 10.1152/ajpcell.00633.2023

68. Parisi L, Toffoli A, Ghezzi B, Mozzoni B, Lumetti S, Macaluso GM. A glance on the role of fibronectin in controlling cell response at biomaterial interface. *J Dent Sci Rev*. 2020;56(1):50-55. doi: 10.1016/j.jdsr.2019.11.002

69. Kupfer ME, Lin WH, Ravikumar V, *et al*. In situ expansion, differentiation, and electromechanical coupling of human cardiac muscle in a 3D bioprinted, chambered organoid. *Circ Res*. 2020;127(2):207-224. doi: 10.1161/CIRCRESAHA.119.316155

70. Ahn S, Jain A, Kasuba KC, *et al*. Engineering fibronectin-templated multi-component fibrillar extracellular matrices to modulate tissue-specific cell response. *Biomaterials*. 2024;308:122560. doi: 10.1016/j.biomaterials.2024.122560

71. Oliver-Cervelló L, Martin-Gómez H, Mas-Moruno C. New trends in the development of multifunctional peptides to functionalize biomaterials. *J Pept Sci*. 2022;28(1):e3335. doi: 10.1002/psc.3335

72. Hersel U, Dahmen C, Kessler H. RGD modified polymers: biomaterials for stimulated cell adhesion and beyond. *Biomaterials*. 2003;24(24):4385-4415. doi: 10.1016/S0142-9612(03)00343-0

73. Xu X, Jha AK, Harrington DA, Farach-Carson MC, Jia X. Hyaluronic acid-based hydrogels: from a natural polysaccharide to complex networks. *Soft Matter*. 2012;8(12):3280. doi: 10.1039/c2sm06463d

74. Bellis SL. Advantages of RGD peptides for directing cell association with biomaterials. *Biomaterials*. 2011;32(18):4205-4210. doi: 10.1016/j.biomaterials.2011.02.029

75. Miner JH, Yurchenco PD. Laminin functions in tissue morphogenesis. *Annu Rev Cell Dev Biol*. 2004;20(1):255-284. doi: 10.1146/annurev.cellbio.20.010403.094555

76. Mota C, Camarero-Espinosa S, Baker MB, Wieringa P, Moroni L. Bioprinting: from tissue and organ development to *in vitro* models. *Chem Rev*. 2020;120(19):10547-10607. doi: 10.1021/acs.chemrev.9b00789

77. He L, Liao S, Quan D, *et al*. The influence of laminin-derived peptides conjugated to Lys-capped PLLA on neonatal mouse cerebellum C17.2 stem cells. *Biomaterials*. 2009;30(8):1578-1586.

doi: 10.1016/j.biomaterials.2008.12.020

78. Penton CM, Badarinarayana V, Prisco J, *et al*. Laminin 521 maintains differentiation potential of mouse and human satellite cell-derived myoblasts during long-term culture expansion. *Skelet Muscle*. 2016;6(1):44. doi: 10.1186/s13395-016-0116-4

79. Aisenbrey EA, Murphy WL. Synthetic alternatives to matrigel. *Nat Rev Mater*. 2020;5(7):539-551. doi: 10.1038/s41578-020-0199-8

80. Speer JE, Barcellona MN, Lu MY, *et al*. Development of a library of laminin-mimetic peptide hydrogels for control of nucleus pulposus cell behaviors. *J Tissue Eng*. 2021;12:20417314211021220. doi: 10.1177/20417314211021220

81. Adams JC. Thrombospondins: conserved mediators and modulators of metazoan extracellular matrix. *Int J Exp Pathol*. 2024;105(5):136-169. doi: 10.1111/iep.12517

82. Calabro NE, Kristofik NJ, Kyriakides TR. Thrombospondin-2 and extracellular matrix assembly. *Biochim Biophys Acta*. 2014;1840(8):2396-2402. doi: 10.1016/j.bbagen.2014.01.013

83. Calabro NE, Barrett A, Chamorro-Jorganes A, *et al*. Thrombospondin-2 regulates extracellular matrix production, LOX levels, and cross-linking via downregulation of miR-29. *Matrix Biol*. 2019;82:71-85. doi: 10.1016/j.matbio.2019.03.002

84. Bornstein P, Kyriakides TR, Yang Z, Armstrong LC, Birk DE. Thrombospondin 2 modulates collagen fibrillogenesis and angiogenesis. *J Investig Dermatol Symp Proc*. 2000;5(1):61-66. doi: 10.1046/j.1087-0024.2000.00005.x

85. Xu ZY, Wang M, Shi JY, *et al*. Engineering a dynamic extracellular matrix using thrombospondin-1 to propel hepatocyte organoids reprogramming and improve mouse liver regeneration post-transplantation. *Mater Today Bio*. 2025;32:101700. doi: 10.1016/j.mtbio.2025.101700

86. Kyriakides TR, MacLauchlan S. The role of thrombospondins in wound healing, ischemia, and the foreign body reaction. *J Cell Commun Signal*. 2009;3(3-4):215-225. doi: 10.1007/s12079-009-0077-z

87. Chen D, Smith LR, Khandekar G, *et al*. Distinct effects of different matrix proteoglycans on collagen fibrillogenesis and cell-mediated collagen reorganization. *Sci Rep*. 2020;10(1):19065. doi: 10.1038/s41598-020-76107-0

88. Iozzo RV, Schaefer L. Proteoglycan form and function: a comprehensive nomenclature of proteoglycans. *Matrix Biol*. 2015;42:11-55. doi: 10.1016/j.matbio.2015.02.003

89. Schönherr E, Hausser HJ. Extracellular matrix and cytokines: a functional unit. *J Immunol Res*. 2000;7(2-4):89-101. doi: 10.1155/2000/31748

90. Nguyen M, Panitch A. Proteoglycans and proteoglycan mimetics for tissue engineering. *Am J Physiol Cell Physiol*. 2022;322(4):C754-C761. doi: 10.1152/ajpcell.00442.2021

91. Wei H, Cui J, Lin K, Xie J, Wang X. Recent advances in smart stimuli-responsive biomaterials for bone therapeutics and regeneration. *Bone Res*. 2022;10(1):17. doi: 10.1038/s41413-021-00180-y

92. Perez S, Makshakova O, Angulo J, *et al*. Glycosaminoglycans: what remains to be deciphered? *JACS Au*. 2023;3(3):628-656. doi: 10.1021/jacsau.2c00569

93. Wang Z, Wang Z, Lu WW, Zhen W, Yang D, Peng S. Novel biomaterial strategies for controlled growth factor delivery for biomedical applications. *NPG Asia Mater*. 2017;9(10):e435-e435. doi: 10.1038/am.2017.171

94. Kempen DHR, Lu L, Heijink A, *et al*. Effect of local sequential VEGF and BMP-2 delivery on ectopic and orthotopic bone regeneration. *Biomaterials*. 2009;30(14):2816-2825. doi: 10.1016/j.biomaterials.2009.01.031

95. Riley LA, Merryman WD. Cadherin-11 and cardiac fibrosis: a common target for a common pathology. *Cell Signal*. 2021;78:109876. doi: 10.1016/j.cellsig.2020.109876

96. Koirala R, Priest AV, Yen CF, *et al*. Inside-out regulation of E-cadherin conformation and adhesion. *Proc Natl Acad Sci U S A*. 2021;118(30):e2104090118. doi: 10.1073/pnas.2104090118

97. Hassan M, Mohanty AK, Wang T, Dhakal HN, Misra M. Current status and future outlook of 4D printing of polymers and composites—a prospective. *Compos Part C Open Access*. 2025;17:100602. doi: 10.1016/j.jcomc.2025.100602

98. Daamen W, Veerkamp J, Vanhest J, Vankuppevelt T. Elastin as a biomaterial for tissue engineering. *Biomaterials*. 2007;28(30):4378-4398. doi: 10.1016/j.biomaterials.2007.06.025

99. Zhu D, Wang H, Trinh P, Heilshorn SC, Yang F. Elastin-like protein-hyaluronic acid (ELP-HA) hydrogels with decoupled mechanical and biochemical cues for cartilage regeneration. *Biomaterials*. 2017;127:132-140. doi: 10.1016/j.biomaterials.2017.02.010

100. Wang H, Zhu D, Paul A, *et al*. Covalently adaptable elastin-like protein–hyaluronic acid (ELP–HA) hybrid hydrogels with secondary thermoresponsive crosslinking for injectable stem cell delivery. *Adv Funct Mater*. 2017;27(28):1605609. doi: 10.1002/adfm.201605609

101. Sugawara-Narutaki A, Nakamura J, Ohtsuki C. Elastin-like hydrogels as tissue regeneration scaffolds. In: *Hydrogels for Tissue Engineering and Regenerative Medicine*. Amsterdam, Netherlands: Elsevier; 2024:65-77.

doi: 10.1016/B978-0-12-823948-3.00018-X

102. Nguyen LT, Odeleye AO, Chui C, Baudequin T, Cui Z, Ye H. Development of thermo-responsive polycaprolactone macrocarriers conjugated with poly(N-isopropyl acrylamide) for cell culture. *Sci Rep*. 2019;9(1):3477. doi: 10.1038/s41598-019-40242-0

103. Trujillo S, Gonzalez-Garcia C, Rico P, *et al*. Engineered 3D hydrogels with full-length fibronectin that sequester and present growth factors. *Biomaterials*. 2020;252:120104. doi: 10.1016/j.biomaterials.2020.120104

104. Namgung S, Kim T, Baik KY, Lee M, Nam J, Hong S. Fibronectin–carbon-nanotube hybrid nanostructures for controlled cell growth. *Small*. 2011;7(1):56-61. doi: 10.1002/smll.201001513

105. Shiwarski DJ, Tashman JW, Tsamis A, *et al*. Fibronectin-based nanomechanical biosensors to map 3D surface strains in live cells and tissue. *Nat Commun*. 2020;11(1):5883. doi: 10.1038/s41467-020-19659-z

106. Silva GA, Czeisler C, Niece KL, *et al*. Selective differentiation of neural progenitor cells by high-epitope density nanofibers. *Science*. 2004;303(5662):1352-1355. doi: 10.1126/science.1093783

107. Ishihara J, Ishihara A, Fukunaga K, *et al*. Laminin heparin-binding peptides bind to several growth factors and enhance diabetic wound healing. *Nat Commun*. 2018;9(1):2163. doi: 10.1038/s41467-018-04525-w

108. Hayes AJ, Farrugia BL, Biose IJ, Bix GJ, Melrose J. Perlecan, a multi-functional, cell-instructive, matrix-stabilizing proteoglycan with roles in tissue development has relevance to connective tissue repair and regeneration. *Front Cell Dev Biol*. 2022;10:856261. doi: 10.3389/fcell.2022.856261

109. Jha AK, Yang W, Kirn-Safran CB, Farach-Carson MC, Jia X. Perlecan domain I-conjugated, hyaluronic acid-based hydrogel particles for enhanced chondrogenic differentiation via BMP-2 release. *Biomaterials*. 2009;30(36):6964-6975. doi: 10.1016/j.biomaterials.2009.09.009

110. Kiani C, Chen L, Wu YJ, Yee AJ, Yang BB. Structure and function of aggrecan. *Cell Res*. 2002;12(1):19-32. doi: 10.1038/sj.cr.7290106

111. Deng Z, Fan T, Xiao C, *et al*. TGF-β signaling in health, disease and therapeutics. *Signal Transduct Target Ther*. 2024;9(1):61. doi: 10.1038/s41392-024-01764-w

112. Rahman MS, Akhtar N, Jamil HM, Banik RS, Asaduzzaman SM. TGF-β/BMP signaling and other molecular events: regulation of osteoblastogenesis and bone formation. *Bone Res*. 2015;3(1):15005. doi: 10.1038/boneres.2015.5

113. Li Y, Liu Y, Bai H, *et al*. Sustained release of VEGF to promote angiogenesis and osteointegration of three-dimensional printed biomimetic titanium alloy implants. *Front Bioeng Biotechnol*. 2021;9:757767. doi: 10.3389/fbioe.2021.757767

114. Schutte RJ, Xie L, Klitzman B, Reichert WM. In vivo cytokine-associated responses to biomaterials. *Biomaterials*. 2009;30(2):160-168. doi: 10.1016/j.biomaterials.2008.09.026

115. Tu Z, Zhong Y, Hu H, *et al*. Design of therapeutic biomaterials to control inflammation. *Nat Rev Mater*. 2022;7(7):557-574. doi: 10.1038/s41578-022-00426-z

116. Barthel SR, Gavino JD, Descheny L, Dimitroff CJ. Targeting selectins and selectin ligands in inflammation and cancer. *Expert Opin Ther Targets*. 2007;11(11):1473-1491. doi: 10.1517/14728222.11.11.1473

117. Pang X, He X, Qiu Z, *et al*. Targeting integrin pathways: mechanisms and advances in therapy. *Signal Transduct Target Ther*. 2023;8(1):1. doi: 10.1038/s41392-022-01259-6

118. Hu M, Ling Z, Ren X. Extracellular matrix dynamics: tracking in biological systems and their implications. *J Biol Eng*. 2022;16(1):13. doi: 10.1186/s13036-022-00292-x

119. Lu P, Weaver VM, Werb Z. The extracellular matrix: a dynamic niche in cancer progression. *J Cell Biol*. 2012;196(4):395-406. doi: 10.1083/jcb.201102147

120. Estrach S, Vivier CM, Féral CC. ECM and epithelial stem cells: the scaffold of destiny. *Front Cell Dev Biol*. 2024;12:1359585. doi: 10.3389/fcell.2024.1359585

121. Kozyrina AN, Piskova T, Di Russo J. Mechanobiology of epithelia from the perspective of extracellular matrix heterogeneity. *Front Bioeng Biotechnol*. 2020;8:596599. doi: 10.3389/fbioe.2020.596599

122. Pfisterer K, Shaw LE, Symmank D, Weninger W. The extracellular matrix in skin inflammation and infection. *Front Cell Dev Biol*. 2021;9:682414. doi: 10.3389/fcell.2021.682414

123. Wagenseil JE, Mecham RP. Vascular extracellular matrix and arterial mechanics. *Physiol Rev*. 2009;89(3):957-989. doi: 10.1152/physrev.00041.2008

124. Burgess JK, Weiss DJ, Westergren-Thorsson G, *et al*. Extracellular matrix as a driver of chronic lung diseases. *Am J Respir Cell Mol Biol*. 2024;70(4):239-246. doi: 10.1165/rcmb.2023-0176PS

125. Del Monte-Nieto G, Fischer JW, Gorski DJ, Harvey RP, Kovacic JC. Basic biology of extracellular matrix in the cardiovascular system, part 1/4. *J Am Coll Cardiol*. 2020;75(17):2169-2188. doi: 10.1016/j.jacc.2020.03.024

126. Luo Y, Li N, Chen H, *et al*. Spatial and temporal changes in extracellular elastin and laminin distribution during lung alveolar development. *Sci Rep*. 2018;8(1):8334. doi: 10.1038/s41598-018-26673-1

127. Mura M, Binnie M, Han B, *et al*. Functions of type II pneumocyte-derived vascular endothelial growth factor in alveolar structure, acute inflammation, and vascular permeability. *Am J Pathol.* 2010;176(4):1725-1734. doi: 10.2353/ajpath.2010.090209

128. Ahmed DW, Tan ML, Liu Y, *et al*. Local photocrosslinking of native tissue matrix regulates lung epithelial cell mechanosensing and function. *Nat Mater*. 2025;24:1812–1825. doi: 10.1038/s41563-025-02329-0

129. Merrilees MJ, Ching PS, Beaumont B, Hinek A, Wight TN, Black PN. Changes in elastin, elastin binding protein and versican in alveoli in chronic obstructive pulmonary disease. *Respir Res*. 2008;9(1):41. doi: 10.1186/1465-9921-9-41

130. Ye X, Gaucher JF, Vidal M, Broussy S. A structural overview of vascular endothelial growth factors pharmacological ligands: from macromolecules to designed peptidomimetics. *Molecules.* 2021;26(22):6759. doi: 10.3390/molecules26226759

131. Csapo R, Gumpenberger M, Wessner B. Skeletal muscle extracellular matrix – what do we know about its composition, regulation, and physiological roles? A narrative review. *Front Physiol*. 2020;11:253. doi: 10.3389/fphys.2020.00253

132. Takala TE, Virtanen P. Biochemical composition of muscle extracellular matrix: the effect of loading. *Scand Med Sci Sports.* 2000;10(6):321-325. doi: 10.1034/j.1600-0838.2000.010006321.x

133. Gillies AR, Lieber RL. Structure and function of the skeletal muscle extracellular matrix. *Muscle Nerve.* 2011;44(3):318-331. doi: 10.1002/mus.22094

134. Stern MM, Myers RL, Hammam N, *et al*. The influence of extracellular matrix derived from skeletal muscle tissue on the proliferation and differentiation of myogenic progenitor cells ex vivo. *Biomaterials.* 2009;30(12):2393-2399. doi: 10.1016/j.biomaterials.2008.12.069

135. Wachsmuth L, Söder S, Fan Z, Finger F, Aigner T. Immunolocalization of matrix proteins in different human cartilage subtypes. *Histol Histopathol*. 2006;(21):477-485. doi: 10.14670/HH-21.477

136. Han B, Li Q, Wang C, *et al*. Decorin regulates the aggrecan network integrity and biomechanical functions of cartilage extracellular matrix. *ACS Nano.* 2019;13(10):11320-11333. doi: 10.1021/acsnano.9b04477

137. McKee TJ, Perlman G, Morris M, Komarova SV. Extracellular matrix composition of connective tissues: a systematic review and meta-analysis. *Sci Rep*. 2019;9(1):10542. doi: 10.1038/s41598-019-46896-0

138. Vainieri ML, Lolli A, Kops N, *et al*. Evaluation of biomimetic hyaluronic-based hydrogels with enhanced endogenous cell recruitment and cartilage matrix formation. *Acta Biomater*. 2020;101:293-303. doi: 10.1016/j.actbio.2019.11.015

139. Fontcuberta-Rigo M, Nakamura M, Puigbò P. Phylobone: a comprehensive database of bone extracellular matrix proteins in human and model organisms. *Bone Res*. 2023;11(1):44. doi: 10.1038/s41413-023-00281-w

140. Qin L, Yang S, Zhao C, *et al*. Prospects and challenges for the application of tissue engineering technologies in the treatment of bone infections. *Bone Res*. 2024;12(1):28. doi: 10.1038/s41413-024-00332-w

141. Hua R, Ni Q, Eliason TD, *et al*. Biglycan and chondroitin sulfate play pivotal roles in bone toughness via retaining bound water in bone mineral matrix. *Matrix Biol.* 2020;94:95-109. doi: 10.1016/j.matbio.2020.09.002

142. Lewns FK, Tsigkou O, Cox LR, Wildman RD, Grover LM, Poologasundarampillai G. Hydrogels and bioprinting in bone tissue engineering: creating artificial stem-cell niches for in vitro models. *Adv Mater*. 2023;35(52):2301670. doi: 10.1002/adma.202301670

143. Silva AC, Pereira C, Fonseca ACRG, Pinto-do-Ó P, Nascimento DS. Bearing my heart: the role of extracellular matrix on cardiac development, homeostasis, and injury response. *Front Cell Dev Biol*. 2021;8:621644. doi: 10.3389/fcell.2020.621644

144. Barallobre-Barreiro J, Loeys B, Mayr M, Rienks M, Verstraeten A, Kovacic JC. Extracellular matrix in vascular disease, part 2/4. *J Am Coll Cardiol.* 2020;75(17): 2189-2203. doi: 10.1016/j.jacc.2020.03.018

145. El-Husseiny HM, Mady EA, El-Dakroury WA, Doghish AS, Tanaka R. Stimuli-responsive hydrogels: smart state of-the-art platforms for cardiac tissue engineering. *Front Bioeng Biotechnol*. 2023;11:1174075. doi: 10.3389/fbioe.2023.1174075

146. Pohl U. Connexins: key players in the control of vascular plasticity and function. *Physiol Rev.* 2020;100(2): 525-572. doi: 10.1152/physrev.00010.2019

147. Davis MJ, Earley S, Li YS, Chien S. Vascular mechanotransduction. *Physiol Rev.* 2023;103(2):1247-1421. doi: 10.1152/physrev.00053.2021

148. Lee TT, García JR, Paez JI, *et al*. Light-triggered in vivo activation of adhesive peptides regulates cell adhesion, inflammation and vascularization of biomaterials. *Nat Mater*. 2015;14(3):352-360. doi: 10.1038/nmat4157

149. Amelung CD, Gerecht S. Cell–material interactions in vascular tissue engineering. *Acc Mater Res*. 2025;6(5):577-588.
doi: 10.1021/accountsmr.4c00390

150. Grigoryan B, Paulsen SJ, Corbett DC, *et al*. Multivascular networks and functional intravascular topologies within biocompatible hydrogels. *Science*. 2019;364(6439):458-464.
doi: 10.1126/science.aav9750

151. Suttkus A, Morawski M, Arendt T. Protective properties of neural extracellular matrix. *Mol Neurobiol*. 2016; 53(1):73-82.
doi: 10.1007/s12035-014-8990-4

152. Chelyshev YA, Kabdesh IM, Mukhamedshina YO. Extracellular matrix in neural plasticity and regeneration. *Cell Mol Neurobiol*. 2022;42(3):647-664.
doi: 10.1007/s10571-020-00986-0

153. Wareham LK, Baratta RO, Del Buono BJ, Schlumpf E, Calkins DJ. Collagen in the central nervous system: contributions to neurodegeneration and promise as a therapeutic target. *Mol Neurodegener*. 2024;19(1):11.
doi: 10.1186/s13024-024-00704-0

154. Weickenmeier J, De Rooij R, Budday S, Steinmann P, Ovaert TC, Kuhl E. Brain stiffness increases with myelin content. *Acta Biomater*. 2016;42:265-272.
doi: 10.1016/j.actbio.2016.07.040

155. Moshayedi P, Ng G, Kwok JC, *et al*. The relationship between glial cell mechanosensitivity and foreign body reactions in the central nervous system. *Biomaterials*. 2014;35(13):3919-3925.
doi: 10.1016/j.biomaterials.2014.01.038

156. Dityatev A, Schachner M, Sonderegger P. The dual role of the extracellular matrix in synaptic plasticity and homeostasis. *Nat Rev Neurosci*. 2010;11(11):735-746.
doi: 10.1038/nrn2898

157. Lam D, Enright HA, Cadena J, *et al*. Tissue-specific extracellular matrix accelerates the formation of neural networks and communities in a neuron-glia co-culture on a multi-electrode array. *Sci Rep*. 2019;9(1):4159.
doi: 10.1038/s41598-019-40128-1

158. Rozario T, DeSimone DW. The extracellular matrix in development and morphogenesis: a dynamic view. *Dev Biol*. 2010;341(1):126-140.
doi: 10.1016/j.ydbio.2009.10.026

159. Muir VG, Burdick JA. Chemically modified biopolymers for the formation of biomedical hydrogels. *Chem Rev*. 2021;121(18):10908-10949.
doi: 10.1021/acs.chemrev.0c00923

160. Joyce K, Fabra GT, Bozkurt Y, Pandit A. Bioactive potential of natural biomaterials: identification, retention and assessment of biological properties. *Signal Transduct Target Ther*. 2021;6(1):122.
doi: 10.1038/s41392-021-00512-8

161. Liu B, Li H, Meng F, *et al*. 4D printed hydrogel scaffold with swelling-stiffening properties and programmable deformation for minimally invasive implantation. *Nat Commun*. 2024;15(1):1587.
doi: 10.1038/s41467-024-45938-0

162. Ni C, Chen D, Yin Y, *et al*. Shape memory polymer with programmable recovery onset. *Nature*. 2023;622(7984):748-753.
doi: 10.1038/s41586-023-06520-8

163. Wang XQ, Chan KH, Lu W, *et al*. Macromolecule conformational shaping for extreme mechanical programming of polymorphic hydrogel fibers. *Nat Commun*. 2022;13(1):3369.
doi: 10.1038/s41467-022-31047-3

164. Yao X, Chen H, Qin H, Wu QH, Cong HP, Yu SH. Solvent-adaptive hydrogels with lamellar confinement cellular structure for programmable multimodal locomotion. *Nat Commun*. 2024;15(1):9254.
doi: 10.1038/s41467-024-53549-y

165. Wang M, Zhang P, Shamsi M, *et al*. Tough and stretchable ionogels by in situ phase separation. *Nat Mater*. 2022;21(3):359-365.
doi: 10.1038/s41563-022-01195-4

166. Kim J, Choi H, Kim Y, Song S. Thermo-responsive nanocomposite bioink with growth-factor holding and its application to bone regeneration. *Small*. 2023;19(9): 2203464.
doi: 10.1002/smll.202203464

167. Parimita S, Kumar A, Krishnaswamy H, Ghosh P. 4D printing of pH-responsive bilayer with programmable shape-shifting behaviour. *Eur Polym J*. 2025;222:113581.
doi: 10.1016/j.eurpolymj.2024.113581

168. Liu J, Huang YS, Liu Y, *et al*. Reconfiguring hydrogel assemblies using a photocontrolled metallopolymer adhesive for multiple customized functions. *Nat Chem*. 2024;16(6):1024-1033.
doi: 10.1038/s41557-024-01476-2

169. Chiesa I, Esposito A, Vozzi G, Gottardi R, De Maria C. 4D bioprinted self-folding scaffolds enhance cartilage formation in the engineering of trachea. *Adv Mater Technol*. 2025;10(6):2401210.
doi: 10.1002/admt.202401210

170. Zhou B, Zou Y, You H, Zhang B, Lu X. Preparation and evaluation of 4D-printed poly(L-lactic) acid/silk fibroin polymer blends with enhanced mechanical properties and water-induced shape memory effects. *Adv Eng Mater*. 2025;27(7):2402496.
doi: 10.1002/adem.202402496

171. Lai J, Xiong T, Chen S, *et al*. Facile single-nanocomposite 4D bioprinting of dynamic hydrogel constructs with thickness-controlled gradient. *Adv Sci*. 2025;12:e09449.
doi: 10.1002/advs.202509449

172. Miao W, Zou W, Jin B, *et al*. On demand shape memory polymer via light regulated topological defects in a dynamic covalent network. *Nat Commun*. 2020;11(1):4257. doi: 10.1038/s41467-020-18116-1

173. Zhang L, Huang X, Cole T, *et al*. 3D-printed liquid metal polymer composites as NIR-responsive 4D printing soft robot. *Nat Commun*. 2023;14(1):7815. doi: 10.1038/s41467-023-43667-4

174. Matsuura K, Inaba H. Photoresponsive peptide materials: spatiotemporal control of self-assembly and biological functions. *Biophys Rev*. 2023;4(4):041303. doi: 10.1063/5.0179171

175. Butenko S, Nagalla RR, Guerrero-Juarez CF, *et al*. Hydrogel crosslinking modulates macrophages, fibroblasts, and their communication, during wound healing. *Nat Commun*. 2024;15(1):6820. doi: 10.1038/s41467-024-50072-y

176. McCracken JM, Rauzan BM, Kjellman JCE, Su H, Rogers SA, Nuzzo RG. Ionic hydrogels with biomimetic 4D-printed mechanical gradients: models for soft-bodied aquatic organisms. *Adv Funct Mater*. 2019;29(28):1806723. doi: 10.1002/adfm.201806723

177. Díaz-Payno PJ, Kalogeropoulou M, Muntz I, *et al*. Swelling-dependent shape-based transformation of a human mesenchymal stromal cells-laden 4D bioprinted construct for cartilage tissue engineering. *Adv Healthc Mater*. 2023;12(2):2201891. doi: 10.1002/adhm.202201891

178. Araújo-Custódio S, Gomez-Florit M, Tomás AR, *et al*. Injectable and magnetic responsive hydrogels with bioinspired ordered structures. *ACS Biomater Sci Eng*. 2019;5(3):1392-1404. doi: 10.1021/acsbiomaterials.8b01179

179. Daul B, Martin R, Glass P, *et al*. 3D printed magnetic origami scaffolds for guided tissue assembly. *Adv Mater Interfaces*. 2025;12:2400903. doi: 10.1002/admi.202400903

180. Zhang H, Hua S, He C, *et al*. Application of 4D-printed magnetoresponsive fogs hydrogel scaffolds in auricular cartilage regeneration. *Adv Healthc Mater*. 2025;14(9):2404488. doi: 10.1002/adhm.202404488

181. Rajan Unnithan A, Krishnamoorthi Kaliannagounder V, Rao Alluri N, Park CH, Veluswamy P, Ramachandra Kurup Sasikala A. Design and application of piezoelectric conductive smart scaffold for noninvasive neural tissue regeneration via custom-made in vitro mechano-stimulator. *Adv Nanobiomed Res*. 2025;5:2500058. doi: 10.1002/anbr.202500058

182. Ebrahimi S, Khoomortezaei S, Fan J, *et al*. Conducting polymer coatings for bioelectronic arthroscopy probes. *Adv Healthc Mater*. 2025;27:e02269. doi: 10.1002/adhm.202502269

183. Liu W, Zhao H, Zhang C, *et al*. In situ activation of flexible magnetoelectric membrane enhances bone defect repair. *Nat Commun*. 2023;14(1):4091. doi: 10.1038/s41467-023-39744-3

184. Yuan Y, Raheja K, Milbrandt NB, *et al*. Thermoresponsive polymers with LCST transition: synthesis, characterization, and their impact on biomedical frontiers. *RSC Appl Polym*. 2023;1(2):158-189. doi: 10.1039/D3LP00114H

185. Qiao SL, Mamuti M, An HW, Wang H. Thermoresponsive polymer assemblies: from molecular design to theranostics application. *Prog Polym Sci*. 2022;131:101578. doi: 10.1016/j.progpolymsci.2022.101578

186. Frazar EM, Shah RA, Dziubla TD, Hilt JZ. Multifunctional temperature-responsive polymers as advanced biomaterials and beyond. *J Appl Polym Sci*. 2020;137(25):48770. doi: 10.1002/app.48770

187. Heskins M, Guillet JE. Solution properties of poly(N-isopropylacrylamide). *J Macromol Sci Part A*. 1968;2(8):1441-1455. doi: 10.1080/10601326808051910

188. Tang Z, Okano T. Recent development of temperature-responsive surfaces and their application for cell sheet engineering. *Regen Biomater*. 2014;1(1):91-102. doi: 10.1093/rb/rbu011

189. Li Z, Zhu Y, Matson JB. pH-responsive self-assembling peptide-based biomaterials: designs and applications. *ACS Appl Bio Mater*. 2022;5(10):4635-4651. doi: 10.1021/acsabm.2c00188

190. Vegad U, Patel M, Khunt D, Zupančič O, Chauhan S, Paudel A. pH stimuli-responsive hydrogels from non-cellulosic biopolymers for drug delivery. *Front Bioeng Biotechnol*. 2023;11:1270364. doi: 10.3389/fbioe.2023.1270364

191. Qu X, Wirsén A, Albertsson AC. Novel pH-sensitive chitosan hydrogels: swelling behavior and states of water. *Polymer*. 2000;41(12):4589-4598. doi: 10.1016/S0032-3861(99)00685-0

192. Zhu L, Bratlie KM. pH sensitive methacrylated chitosan hydrogels with tunable physical and chemical properties. *Biochem Eng J*. 2018;132:38-46. doi: 10.1016/j.bej.2017.12.012

193. Ollier RC, Webber MJ. Mechanoresponsive hydrogels emerging from dynamic and non-covalent interactions. *Adv Mater*. 2025;37(40):2507397. doi: 10.1002/adma.202507397

194. Yang EC, Divine R, Miranda MC, *et al*. Computational design of non-porous pH-responsive antibody nanoparticles. *Nat Struct Mol Biol*. 2024;31(9):1404-1412. doi: 10.1038/s41594-024-01288-5

195. Mintis DG, Mavrantzas VG. Effect of pH and molecular length on the structure and dynamics of short poly(acrylic

acid) in dilute solution: detailed molecular dynamics study. *J Phys Chem B.* 2019;123(19):4204-4219. doi: 10.1021/acs.jpcb.9b01696

196. Farasati Far B, Omrani M, Naimi Jamal MR, Javanshir S. Multi-responsive chitosan-based hydrogels for controlled release of vincristine. *Commun Chem*. 2023;6(1):28. doi: 10.1038/s42004-023-00829-1

197. Zoe LH, David SR, Rajabalaya R. Chitosan nanoparticle toxicity: a comprehensive literature review of in vivo and in vitro assessments for medical applications. *Toxicol Rep.* 2023;11:83-106. doi: 10.1016/j.toxrep.2023.06.012

198. Shin Y, Kim D, Hu Y, *et al*. pH-responsive succinoglycan-carboxymethyl cellulose hydrogels with highly improved mechanical strength for controlled drug delivery systems. *Polymers.* 2021;13(18):3197. doi: 10.3390/polym13183197

199. Héraly F, Zhang M, Åhl A, Cao W, Bergström L, Yuan J. Nanodancing with moisture: humidity-sensitive bilayer actuator derived from cellulose nanofibrils and reduced graphene oxide. *Adv Intell Syst*. 2022;4(1):2100084. doi: 10.1002/aisy.202100084

200. Guo F, Kim F, Han TH, Shenoy VB, Huang J, Hurt RH. Hydration-responsive folding and unfolding in graphene oxide liquid crystal phases. *ACS Nano.* 2011;5(10):8019-8025. doi: 10.1021/nn2025644

201. Formisano N, Van Der Putten C, Grant R, *et al*. Mechanical properties of bioengineered corneal stroma. *Adv Healthc Mater*. 2021;10(20):2100972. doi: 10.1002/adhm.202100972

202. Pérez-Madrigal MM, Shaw JE, Arno MC, Hoyland JA, Richardson SM, Dove AP. Robust alginate/hyaluronic acid thiol-yne click-hydrogel scaffolds with superior mechanical performance and stability for load-bearing soft tissue engineering. *Biomater Sci.* 2020;8(1):405-412. doi: 10.1039/C9BM01494B

203. Jamilludin MA, Dinatha IKH, Supii AI, Partini J, Kusindarta DL, Yusuf Y. Functionalized cellulose nanofibrils in carbonate-substituted hydroxyapatite nanorod-based scaffold from long-spined sea urchin (*Diadema setosum*) shells reinforced with polyvinyl alcohol for alveolar bone tissue engineering. *RSC Adv*. 2023;13(46):32444-32456. doi: 10.1039/D3RA06165E

204. Lawless BM, Sadeghi H, Temple DK, Dhaliwal H, Espino DM, Hukins DWL. Viscoelasticity of articular cartilage: analysing the effect of induced stress and the restraint of bone in a dynamic environment. *J Mech Behav Biomed Mater.* 2017;75:293-301. doi: 10.1016/j.jmbbm.2017.07.040

205. Lee HP, Gaharwar AK. Light-responsive inorganic biomaterials for biomedical applications. *Adv Sci*. 2020;7(17):2000863. doi: 10.1002/advs.202000863

206. Chen G, Cao Y, Tang Y, *et al*. Advanced near-infrared light for monitoring and modulating the spatiotemporal dynamics of cell functions in living systems. *Adv Sci*. 2020;7(8):1903783. doi: 10.1002/advs.201903783

207. Lu Y, Chen C, Li H, *et al*. Visible light-responsive hydrogels for cellular dynamics and spatiotemporal viscoelastic regulation. *Nat Commun*. 2025;16(1):1365. doi: 10.1038/s41467-024-54880-0

208. Guo P, Dong L, Xue B, Cao Y, Yang J. From light to life: molecular mechanisms and macroscopic transformations in photoresponsive hydrogels. *Polym Sci Technol.* 2025;1:812−831. doi: 10.1021/polymscitech.5c00102

209. Overchuk M, Weersink RA, Wilson BC, Zheng G. Photodynamic and photothermal therapies: synergy opportunities for nanomedicine. *ACS Nano.* 2023;17(9):7979-8003. doi: 10.1021/acsnano.3c00891

210. Jayakumar MKG, Idris NM, Zhang Y. Remote activation of biomolecules in deep tissues using near-infrared-to-UV upconversion nanotransducers. *Proc Natl Acad Sci U S A.* 2012;109(22):8483-8488. doi: 10.1073/pnas.1114551109

211. Liu TM, Conde J, Lipiński T, Bednarkiewicz A, Huang CC. Revisiting the classification of nir-absorbing/emitting nanomaterials for in vivo bioapplications. *NPG Asia Mater*. 2016;8(8):e295-e295. doi: 10.1038/am.2016.106

212. Lee CH, Wu SB, Hong CH, Yu HS, Wei YH. Molecular mechanisms of UV-induced apoptosis and its effects on skin residential cells: the implication in UV-Based Phototherapy. *Int J Mol Sci.* 2013;14(3):6414-6435. doi: 10.3390/ijms14036414

213. Meng F, Meyer CM, Joung D, Vallera DA, McAlpine MC, Panoskaltsis-Mortari A. 3D bioprinted in vitro metastatic models via reconstruction of tumor microenvironments. *Adv Mater*. 2019;31(10):1806899. doi: 10.1002/adma.201806899

214. He D, Zhao A, Su H, *et al*. An injectable scaffold based on temperature-responsive hydrogel and factor-loaded nanoparticles for application in vascularization in tissue engineering. *J Biomed Mater Res.* 2019;107(10): 2123-2134. doi: 10.1002/jbm.a.36723

215. Bonnet S. Ruthenium-based photoactivated chemotherapy. *J Am Chem Soc*. 2023;145(43):23397-23415. doi: 10.1021/jacs.3c01135

216. Munteanu AC, Notaro A, Jakubaszek M, *et al*. Synthesis, characterization, cytotoxic activity, and metabolic studies of ruthenium(II) polypyridyl complexes containing flavonoid ligands. *Inorg Chem*. 2020;59(7):4424-4434. doi: 10.1021/acs.inorgchem.9b03562

217. António JPM, Gandioso A, Nemati F, *et al*. Polymeric encapsulation of a ruthenium(II) polypyridyl complex: from synthesis to *in vivo* studies against high-grade epithelial ovarian cancer. *Chem Sci*. 2023;14(2):362-371. doi: 10.1039/D2SC05693C

218. Bolanta SO, Malijauskaite S, McGourty K, O'Reilly EJ. Synthesis of poly(acrylic acid)-cysteine-based hydrogels with highly customizable mechanical properties for advanced cell culture applications. *ACS Omega*. 2022;7(11):9108-9117. doi: 10.1021/acsomega.1c03408

219. Suhail M, Liu JY, Hung MC, Chiu IH, Minhas MU, Wu PC. Preparation, in vitro characterization, and cytotoxicity evaluation of polymeric pH-responsive hydrogels for controlled drug release. *Pharmaceutics*. 2022;14(9):1864. doi: 10.3390/pharmaceutics14091864

220. Leigh BL, Cheng E, Xu L, Derk A, Hansen MR, Guymon CA. Antifouling photograftable zwitterionic coatings on PDMS substrates. *Langmuir*. 2019;35(5):1100-1110. doi: 10.1021/acs.langmuir.8b00838

221. Zhao C, Zheng J. Synthesis and characterization of poly(*N*-hydroxyethylacrylamide) for long-term antifouling ability. *Biomacromolecules*. 2011;12(11):4071-4079. doi: 10.1021/bm2011455

222. Fernandes LC, Correia DM, Costa CM, Lanceros-Mendez S. Recent advances in ionic liquid-based hybrid materials for electroactive soft actuator applications. *Macromol Mater Eng*. 2025;310(2):2400279. doi: 10.1002/mame.202400279

223. Datta D, Colaco V, Bandi SP, *et al*. Stimuli-responsive self-healing ionic gels: a promising approach for dermal and tissue engineering applications. *ACS Biomater Sci Eng*. 2025;11(3):1338-1372. doi: 10.1021/acsbiomaterials.4c02264

224. Plaas AHK, Moran MM, Sandy JD, Hascall VC. Aggrecan and hyaluronan: the infamous cartilage polyelectrolytes – then and now. In: Connizzo BK, Han L, Sah RL, eds. *Electromechanobiology of Cartilage and Osteoarthritis*. Vol. 1402. Advances in Experimental Medicine and Biology. Cham, Switzerland: Springer International Publishing; 2023:3-29. doi: 10.1007/978-3-031-25588-5_1

225. Ricka J, Tanaka T. Swelling of ionic gels: quantitative performance of the Donnan theory. *Macromolecules*. 1984;17(12):2916-2921. doi: 10.1021/ma00142a081

226. Wei W. Hofmeister effects shine in nanoscience. *Adv Sci*. 2023;10(22):2302057. doi: 10.1002/advs.202302057

227. Huang S, Zhao Z, Feng C, Mayes E, Yang J. Nanocellulose reinforced P(AAm-co-AAc) hydrogels with improved mechanical properties and biocompatibility. *Compos A Appl Sci Manuf*. 2018;112:395-404. doi: 10.1016/j.compositesa.2018.06.028

228. Echeverria C, Fernandes SN, Godinho MH, Borges JP, Soares PIP. Functional stimuli-responsive gels: hydrogels and microgels. *Gels*. 2018;4(2):54. doi: 10.3390/gels4020054

229. Chen H, Wei P, Qi Y, Xie Y, Huang X. Water-induced cellulose nanofibers/poly(vinyl alcohol) hydrogels regulated by hydrogen bonding for in situ water shutoff. *ACS Appl Mater Interfaces*. 2023;15(33):39883-39895. doi: 10.1021/acsami.3c07989

230. Xu W, Newton MAA, Chen Z, Xin B. Design, characterization, and performance evaluation of novel PVA/CS/CNF/MOP TN ionic conductive hydrogels for flexible sensors. *J Polym Sci*. 2024;62(12):2744-2761. doi: 10.1002/pol.20240043

231. Zhang H, Fu C, Yong LC, Sun N, Liu FG. Flexible and transparent PVA/CNF hydrogel with ultrahigh dielectric constant. *ACS Appl Polym Mater*. 2024;6(10):5706-5713. doi: 10.1021/acsapm.4c00302

232. Xu Z, Chen H, Yang HB, *et al*. Hierarchically aligned heterogeneous core-sheath hydrogels. *Nat Commun*. 2025;16(1):400. doi: 10.1038/s41467-024-55677-x

233. Zhang A, Yue Z, Grove B, *et al*. Highly-soft, scalable, personalizable skin-interfaced systems via self-healing gels. *Adv Funct Mater*. 2025;35(50):e07821. doi: 10.1002/adfm.202507821

234. Mistral J, Ve Koon KT, Fernando Cotica L, *et al*. Chitosan-coated superparamagnetic Fe_3O_4 nanoparticles for magnetic resonance imaging, magnetic hyperthermia, and drug delivery. *ACS Appl Nano Mater*. 2024;7(7):7097-7110. doi: 10.1021/acsanm.3c06118

235. Mammoto A, Mammoto T, Ingber DE. Mechanosensitive mechanisms in transcriptional regulation. *J Cell Sci*. 2012:125 (13): 3061–3073. doi: 10.1242/jcs.093005

236. Lucariello M, Valicenti ML, Giannoni S, *et al*. Mechanobiology in action: biomaterials, devices, and the cellular machinery of force sensing. *Biomolecules*. 2025;15(6):848. doi: 10.3390/biom15060848

237. Estelrich J, Busquets MA, Del Carmen Morán M. Effect of PEGylation on ligand-targeted magnetoliposomes: a missed goal. *ACS Omega*. 2017;2(10):6544-6555. doi: 10.1021/acsomega.7b00778

238. Masoumi Godgaz S, Asefnejad A, Bahrami SH. Fabrication of PEGylated SPIONs-loaded niosome for codelivery of paclitaxel and trastuzumab for breast cancer treatment: in vivo study. *ACS Appl Bio Mater*. 2024;7(5):2951-2965. doi: 10.1021/acsabm.4c00027

239. Carter TJ, Agliardi G, Lin F, *et al*. Potential of magnetic hyperthermia to stimulate localized immune activation. *Small*. 2021;17(14):2005241.

doi: 10.1002/smll.202005241

240. Moonesi Rad R, Daul B, Glass P, *et al*. 3D printed magnet-infused origami platform for 3D cell culture assessments. *Adv Mater Technol*. 2023;8(8):2202204. doi: 10.1002/admt.202202204

241. Yang D, Hu Y, Liu S, *et al*. Synthesis and assembly strategy of electroactive biomaterials and systems for soft tissue engineering applications. *Chem*. 2025;11(9):102596. doi: 10.1016/j.chempr.2025.102596

242. Ning C, Zhou Z, Tan G, Zhu Y, Mao C. Electroactive polymers for tissue regeneration: Developments and perspectives. *Prog Polym Sci*. 2018;81:144-162. doi: 10.1016/j.progpolymsci.2018.01.001

243. Chen AY, Pegg E, Chen A, Jin Z, Gu GX. 4D printing of electroactive materials. *Adv Intell Syst*. 2021;3(12):2100019. doi: 10.1002/aisy.202100019

244. Grodzinsky AJ. Electromechanical and physicochemical properties of connective tissue. *Crit Rev Biomed Eng*. 1983;9(2):133-199. doi: 10.1016/0021-9290(87)90282-x.

245. Pillay V, Tsai T, Choonara YE, *et al*. A review of integrating electroactive polymers as responsive systems for specialized drug delivery applications. *J Biomed Mater Res*. 2014;102(6):2039-2054. doi: 10.1002/jbm.a.34869

246. Acharya R, Dutta SD, Patil TV, Ganguly K, Randhawa A, Lim KT. A review on electroactive polymer–metal composites: development and applications for tissue regeneration. *J Funct Biomater*. 2023;14(10):523. doi: 10.3390/jfb14100523

247. Rivnay J, Inal S, Collins BA, *et al*. Structural control of mixed ionic and electronic transport in conducting polymers. *Nat Commun*. 2016;7(1):11287. doi: 10.1038/ncomms11287

248. Deng X, Zhuang Y, Cui J, *et al*. Open challenges and opportunities in piezoelectricity for tissue regeneration. *Adv Sci*. 2025;12(38):e10349. doi: 10.1002/advs.202510349

249. Filippi M, Badolato A, Georgopoulou A, *et al*. Bioprinting of piezoresistive organohydrogel networks for advanced real-time mechanosensing in engineered tissue models. *Trends Biotechnol*. 2025;43(10):2509-2538. doi: 10.1016/j.tibtech.2025.05.026

250. Faber L, Yau A, Chen Y. Translational biomaterials of four-dimensional bioprinting for tissue regeneration. *Biofabrication*. 2024;16(1):012001. doi: 10.1088/1758-5090/acfdd0

251. Narayana S, Gowda BHJ, Hani U, Ahmed MG, Asiri ZA, Paul K. Smart poly(N-isopropylacrylamide)-based hydrogels: a tour d'horizon of biomedical applications. *Gels*. 2025;11(3):207. doi: 10.3390/gels11030207

252. Cui Z, Lee BH, Pauken C, Vernon BL. Degradation, cytotoxicity, and biocompatibility of NIPAAm-based thermosensitive, injectable, and bioresorbable polymer hydrogels. *J Biomed Mater Res*. 2011;98A(2):159-166. doi: 10.1002/jbm.a.33093

253. Allyn MM, Luo RH, Hellwarth EB, Swindle-Reilly KE. Considerations for polymers used in ocular drug delivery. *Front Med*. 2022;8:787644. doi: 10.3389/fmed.2021.787644

254. Chu S, Shi X, Tian Y, Gao F. pH-responsive polymer nanomaterials for tumor therapy. *Front Oncol*. 2022;12:855019. doi: 10.3389/fonc.2022.855019

255. Gao W, Chan JM, Farokhzad OC. pH-responsive nanoparticles for drug delivery. *Mol Pharm*. 2010;7(6):1913-1920. doi: 10.1021/mp100253e

256. Linsley CS, Wu BM. Recent advances in light-responsive on-demand drug-delivery systems. *Ther Deliv*. 2017;8(2):89-107. doi: 10.4155/tde-2016-0060

257. Verbroekken RMC, Savchak OK, Alofs TFJ, Schenning APHJ, Gumuscu B. Light-responsive liquid crystal surface topographies for dynamic stimulation of cells. *ACS Appl Mater Interfaces*. 2025;17(19):27871-27881. doi: 10.1021/acsami.5c02526

258. Lungu CN, Gurau G, Mehedinti MC. Pro-angiogenic bioactive molecules in vascular morphogenesis: integrating endothelial cell dynamics. *Curr Issues Mol Biol*. 2025;47(10):851. doi: 10.3390/cimb47100851

259. Bril M, Saberi A, Jorba I, *et al*. Shape-morphing photoresponsive hydrogels reveal dynamic topographical conditioning of fibroblasts. *Adv Sci*. 2023;10(31):2303136. doi: 10.1002/advs.202303136

260. Li C, Iscen A, Palmer LC, Schatz GC, Stupp SI. Light-driven expansion of spiropyran hydrogels. *J Am Chem Soc*. 2020;142(18):8447-8453. doi: 10.1021/jacs.0c02201

261. Yue K, Trujillo-de Santiago G, Alvarez MM, Tamayol A, Annabi N, Khademhosseini A. Synthesis, properties, and biomedical applications of gelatin methacryloyl (GelMA) hydrogels. *Biomaterials*. 2015;73:254-271. doi: 10.1016/j.biomaterials.2015.08.045

262. Nowak BP, Niehues M, Ravoo BJ. Magneto-responsive hydrogels by self-assembly of low molecular weight peptides and crosslinking with iron oxide nanoparticles. *Soft Matter*. 2021;17(10):2857-2864. doi: 10.1039/D0SM02049D

263. Hu K, Yu T, Tang S, *et al*. Dual anisotropicity comprising 3D printed structures and magnetic nanoparticle assemblies: towards the promotion of mesenchymal stem cell osteogenic differentiation. *NPG Asia Mater*. 2021;13(1):19. doi: 10.1038/s41427-021-00288-x

264. Malektaj H, Drozdov AD, deClaville Christiansen J. Mechanical properties of alginate hydrogels cross-linked with multivalent cations. *Polymers.* 2023;15(14):3012. doi: 10.3390/polym15143012

265. Salari P, Easson GWD, Broz KS, Kelly MP, Tang SY. Effects of sustained tensile distraction on vertebrae and intervertebral disc growth: an in vivo study using a mouse tail model. *J Bone Joint Surg Am*. 2025;107(10):1107-1115. doi: 10.2106/JBJS.24.00224

266. Freeman FE, Kelly DJ. Tuning alginate bioink stiffness and composition for controlled growth factor delivery and to spatially direct MSC fate within bioprinted tissues. *Sci Rep*. 2017;7(1):17042. doi: 10.1038/s41598-017-17286-1

267. Meyers K, Lee BP, Rajachar RM. Electroactive polymeric composites to mimic the electromechanical properties of myocardium in cardiac tissue repair. *Gels*. 2021;7(2):53. doi: 10.3390/gels7020053

268. Roshanbinfar K, Schiffer M, Carls E, *et al*. Electrically conductive collagen-PEDOT:PSS hydrogel prevents post-infarct cardiac arrhythmia and supports hiPSC-cardiomyocyte function. *Adv Mater*. 2024;36(28):2403642. doi: 10.1002/adma.202403642

269. Jebran AF, Seidler T, Tiburcy M, *et al*. Engineered heart muscle allografts for heart repair in primates and humans. *Nature*. 2025;639(8054):503-511. doi: 10.1038/s41586-024-08463-0

270. Zhu J. Bioactive modification of poly(ethylene glycol) hydrogels for tissue engineering. *Biomaterials*. 2010;31(17):4639-4656. doi: 10.1016/j.biomaterials.2010.02.044

271. Patel DK, Jung E, Priya S, Won SY, Han SS. Recent advances in biopolymer-based hydrogels and their potential biomedical applications. *Carbohydr Polym*. 2024;323:121408. doi: 10.1016/j.carbpol.2023.121408

272. Sexton ZA, Rütsche D, Herrmann JE, *et al*. Rapid model-guided design of organ-scale synthetic vasculature for biomanufacturing. *Science*. 2025;388(6752):1198-1204. doi: 10.1126/science.adj6152

273. Chen Z, Wang Y, Chen H, *et al*. A magnetic multi-layer soft robot for on-demand targeted adhesion. *Nat Commun*. 2024;15(1):644. doi: 10.1038/s41467-024-44995-9

274. Pang X, Liang S, Wang T, *et al*. Engineering thermo-pH dual responsive hydrogel for enhanced tumor accumulation, penetration, and chemo-protein combination therapy. *Int J Nanomed*. 2020;15:4739-4752. doi: 10.2147/IJN.S253990

275. Kumar K, Nain A. Emerging 4D fabrication of tubular structures and clinical challenges: critical perspective. *ACS Mater Au*. 2025;5(6):886-895. doi: 10.1021/acsmaterialsau.5c00101

276. Huang G, Zhao Y, Chen D, *et al*. Applications, advancements, and challenges of 3D bioprinting in organ transplantation. *Biomater Sci*. 2024;12(6):1425-1448. doi: 10.1039/D3BM01934A

277. Osouli-Bostanabad K, Masalehdan T, Kapsa RM, *et al*. Traction of 3D and 4D printing in the healthcare industry: from drug delivery and analysis to regenerative medicine. *ACS Biomater Sci Eng*. 2022;8(7):2764-2797. doi: 10.1021/acsbiomaterials.2c00094

278. Ramesh S, Harrysson OLA, Rao PK, *et al*. Extrusion bioprinting: recent progress, challenges, and future opportunities. *Bioprinting*. 2021;21:e00116. doi: 10.1016/j.bprint.2020.e00116

279. Li MX, Wei QQ, Mo HL, *et al*. Challenges and advances in materials and fabrication technologies of small-diameter vascular grafts. *Biomater Res*. 2023;27(1):58. doi: 10.1186/s40824-023-00399-2

280. Sun J, Gong Y, Xu M, Chen H, Shao H, Zhou R. Coaxial 3D bioprinting process research and performance tests on vascular scaffolds. *Micromachines*. 2024;15(4):463. doi: 10.3390/mi15040463

281. Damiati LA, Alsudir SA, Mohammed RY, *et al*. 4D printing in skin tissue engineering: a revolutionary approach to enhance wound healing and combat infections. *Bioprinting*. 2025;45:e00386. doi: 10.1016/j.bprint.2025.e00386

282. Bonatti AF, Batoni E, Fortunato GM, Vitale-Brovarone C, Vozzi G, De Maria C. Robust design methodologies to engineer multimaterial and multiscale bioprinters. *Bioprinting*. 2024;44:e00372. doi: 10.1016/j.bprint.2024.e00372

283. Albrecht FB, Schmidt FF, Schmidt C, Börret R, Kluger PJ. Robot-based 6D bioprinting for soft tissue biomedical applications. *Eng Life Sci*. 2024;24(7):e2300226. doi: 10.1002/elsc.202300226

284. Pettersson ABV, Ballardini RM, Mimler M, *et al*. Core legal challenges for medical 3D printing in the EU. *Healthcare*. 2024;12(11):1114. doi: 10.3390/healthcare12111114

285. Gilbert F, O'Connell CD, Mladenovska T, Dodds S. Print me an organ? Ethical and regulatory issues emerging from 3D bioprinting in medicine. *Sci Eng Ethics*. 2018;24(1):73-91. doi: 10.1007/s11948-017-9874-6

286. Ricles LM, Coburn JC, Di Prima M, Oh SS. Regulating 3D-printed medical products. *Sci Transl Med*. 2018;10(461):eaan6521. doi: 10.1126/scitranslmed.aan6521

287. U.S. Food and Drug Administration. 21 CFR Part 1271—Human cells, tissues, and cellular and tissue-based products. Code of Federal Regulations; 2024. https://www.ecfr.gov/current/title-21/chapter-I/subchapter-L/part-1271

288. U.S. Food and Drug Administration. Classification of products as drugs and devices and additional product classification issues: Guidance for industry and FDA staff (Footnote 12); 2017
https://www.fda.gov/regulatory-information/search-fda-guidance-documents/classification-products-drugs-and-devices-and-additional-product-classification-issues

289. Vijayavenkataraman S, Lu WF, Fuh JYH. 3D bioprinting – an ethical, legal and social aspects (ELSA) framework. *Bioprinting*. 2016;1-2:11-21.
doi: 10.1016/j.bprint.2016.08.001

290. Melvin T. The European medical device regulation–what biomedical engineers need to know. *IEEE J Transl Eng Health Med*. 2022;10:1-5.
doi: 10.1109/JTEHM.2022.3194415

291. European Parliament & Council. Regulation (EC) No 1394/2007 on advanced therapy medicinal products, OJ L. 2007;324:121–137.
https://eur-lex.europa.eu/eli/reg/2007/1394/oj/eng

292. Dwenger A, Straßburger J, Schwerdtfeger W. Regulation (EC) No. 1394/2007 on advanced therapy medicinal products: incorporation into national law. *Bundesgesundheitsblatt Gesundheitsforschung Gesundheitsschutz*. 2010;53(1):14-19.
doi: 10.1007/s00103-009-0985-3

293. Kim M, Kim YJ, Kim YS, *et al*. One-year results of ear reconstruction with 3d printed implants. *Yonsei Med J*. 2024;65(8):456.
doi: 10.3349/ymj.2023.0444

294. World Health Organization. Considerations in developing a regulatory framework for human cells and tissues and for advanced therapy medicinal products (TRS 1048, Annex 3); 2023.
https://www.who.int/publications/m/item/considerations-in-developing-a-regulatory-framework-for-human-cells-and-tissues-and-for-advanced-therapy-medicinal-products

295. Human Tissue Act 2004, c. 30. (2004). UK Public General Acts.
https://www.legislation.gov.uk/ukpga/2004/30/contents